

A new Oligo–Miocene marsupial lion from Australia and revision of the family Thylacoleonidae

Anna K. Gillespie, Michael Archer & Suzanne J. Hand

To cite this article: Anna K. Gillespie, Michael Archer & Suzanne J. Hand (2017): A new Oligo–Miocene marsupial lion from Australia and revision of the family Thylacoleonidae, *Journal of Systematic Palaeontology*, DOI: [10.1080/14772019.2017.1391885](https://doi.org/10.1080/14772019.2017.1391885)

To link to this article: <https://doi.org/10.1080/14772019.2017.1391885>

 View supplementary material [↗](#)

 Published online: 06 Dec 2017.

 Submit your article to this journal [↗](#)

 View related articles [↗](#)

 View Crossmark data [↗](#)



A new Oligo–Miocene marsupial lion from Australia and revision of the family Thylacoleonidae

Anna K. Gillespie*, Michael Archer and Suzanne J. Hand

PANGEA Research Centre, School of Biological, Earth and Environmental Sciences,
University of New South Wales, Sydney 2052, Australia

(Received 28 May 2017; accepted 19 September 2017; published online 7 December 2017)

Wakaleo schouteni sp. nov., a dog-sized marsupial lion (Thylacoleonidae), is described from late Oligocene to early Miocene sediments of the Riversleigh World Heritage Area, Queensland, Australia. Fossils of this new species include a near-complete cranium, dentaries and postcrania. This species is the second thylacoleonid known from late Oligocene sediments. The other, *Priscileo pitikantensis* Rauscher, 1987, from the Etadunna Formation of South Australia, is known from teeth, part of a palate and postcrania. *Wakaleo schouteni* exhibits cranial and dental morphology characteristic of species of *Wakaleo* but possesses a relatively plesiomorphic upper dental formula (i.e. three premolars and four molars) within Thylacoleonidae that was formerly regarded to be diagnostic for species of the genus *Priscileo*. The holotype and humerus of *P. pitikantensis* have been compared with the new *Wakaleo* material described here and found to demonstrate conspicuous similarities in morphology of the M² and the humerus. In the absence of other generically diagnostic features, *Priscileo* is here regarded to be a junior synonym of *Wakaleo*. Smaller size and relatively minor morphological differences in the proximal humerus of *W. pitikantensis* comb. nov. distinguish it at the specific level from *W. schouteni*. Phylogenetic analysis of thylacoleonids recovers *Wakaleo* as a monophyletic clade. Both *Wakaleo pitikantensis* comb. nov. and *W. schouteni* are recovered as plesiomorphic sister taxa to other species of the genus. *Wakaleo pitikantensis* and *W. schouteni* extend the temporal range for this genus back into the late Oligocene. Body weight for *W. schouteni*, based on total skull length, is estimated to be ~23 kg.

<http://zoobank.org/urn:lsid:zoobank.org:pub:CA8A8EC8-4F66-4F1E-81DC-240A0C4080BE>

Keywords: marsupial lion; Thylacoleonidae; Oligocene–Miocene; taxonomy; *Priscileo*; Riversleigh

Introduction

Thylacoleonidae is a family of extinct marsupials, many of which were probably peak mammalian carnivores in later Cenozoic faunas of Australia. The family is characterized dentally by the development of the posteriormost premolars (P³/₃) into elongate, sectorial blades, the extreme hypertrophy of which in the Pleistocene species, *Thylacoleo carnifex*, led Sir Richard Owen (1859, p. 319) to describe it as “...one of the fellest and most destructive of predatory beasts.”

The family contains four genera and nine species. Three of the genera are known from late Oligocene to Miocene deposits: *Wakaleo* Clemens & Plane, 1974; *Priscileo* Rauscher, 1987; and *Microleo* Gillespie *et al.*, 2016. The first is comprised of species of medium to large dog-sized marsupial lions that exhibit loss of the anterior premolars and posterior molars. Fossils of this genus are not common. *Wakaleo oldfieldi* is known from limited dental material collected from the early Miocene Kutjamarpu

Local Fauna (LF), Lake Ngapakaldi, in South Australia (Clemens & Plane 1974) and five localities in the Riversleigh World Heritage Area (WHA) of north-western Queensland (Gillespie *et al.* 2014). The slightly larger species, *Wakaleo vanderleueri*, is known from a cranium, dentaries and teeth recovered from the middle Miocene Bullock Creek LF in the Northern Territory (Clemens & Plane 1974; Megirian 1986; Murray *et al.* 1987; Murray & Megirian 1990) and from the possibly early late Miocene Encore and Golden Steph LFs in the Riversleigh WHA (Gillespie *et al.* 2014). *Wakaleo alcootaensis* is the largest and youngest species of the genus and is known from a single maxillary fragment, two dentary fragments and isolated teeth recovered from the late Miocene Alcoota LF in the Northern Territory (Archer & Rich 1982; Yates 2015). *Priscileo* until now has been regarded to contain two species: *P. pitikantensis* from the late Oligocene Ngapakaldi LF, Lake Pitikanta, of South Australia (Rauscher 1987; Fig. 1) which is known from a partial palate with one tooth and a few postcranial bones;

*Corresponding author. Email: a.gillespie@unsw.edu.au

and *P. roskellyae* from early Miocene LFs of the Riversleigh WHA (Gillespie 1997), which is known from cranial and dental material. The monotypic *Microleo* contains the rare and diminutive species *M. attenboroughi*, also from the Early Miocene of Riversleigh (Gillespie *et al.* 2016).

This paper describes the skull, lower dentition and humerus of a new species of *Wakaleo*, *W. schouteni*, recovered from late Oligocene–middle Miocene limestones of the Riversleigh WHA (Fig. 1). This new material shares many dental and cranial features with *W. oldfieldi* and *W. vanderleueri* that support its referral to the genus *Wakaleo* but it also exhibits a number of

similarities to *P. pitikantensis*, the most significant being the diagnostic feature of the genus *Priscileo*, presence of three premolars and four molars. Previously, the major features used to distinguish species of *Wakaleo* from those of *Priscileo* have been larger size and the loss of anterior premolars and posterior molars (Murray *et al.* 1987; Rauscher 1987; Gillespie 1997). These dental attributes, as well as its similarity in size to the new species of *Wakaleo*, have prompted a reassessment below of the generic distinction of *pitikantensis* (SAM P37719), a rediagnosis of the genus *Wakaleo* and a phylogenetic analysis of thylacoleonid relationships based on craniodental features.



Figure 1. Map of Australia showing the location of the Riversleigh World Heritage Area and Lake Pitikanta.

Material and methods

The material described from the Riversleigh WHA is part of the palaeontology collection of the Queensland Museum, Brisbane. Material of *Priscileo pitikantensis* is held in the Palaeontology collection of the South Australian Museum, Adelaide. The holotype of *P. pitikantensis* (SAM P37719) was compared to craniodental material of species of *Wakaleo*, *Priscileo* and *Thylacoleo carnifex*. To investigate intraspecific and interspecific variation in marsupial humeri, samples of the humeri of *Thylacoleo carnifex* (13), *Phascolarctos cinereus* (22) *Trichosurus vulpecula* (23), *Tr. caninus* (6) and *Spilocuscus maculatus* (4) were examined. Measurements were made of the sample of *Thylacoleo carnifex* humeri to obtain an estimate of variation in a population of thylacoleonids; 12 of the 13 humeri in the sample are from localities in South Australia, the majority from Naracoorte Caves (11 of 12). A list of all craniodental and postcranial specimens examined is provided in the Supplemental material. Measurements were made to the nearest 0.1 mm using dial callipers.

Phylogenetic analysis

Rauscher (1987) presented a cladogram of thylacoleonid relationships, placing *Priscileo* as the sister taxon to a *Wakaleo* + *Thylacoleo* clade. This phylogeny was based on a restricted number of craniodental characters and was not generated by a computer based parsimony program. We used PAUP * 4.0b10 (Swofford 2002) to assess the phylogenetic relationships of species of *Wakaleo* and *Priscileo*, based on a modified data matrix of Gillespie *et al.* (2016). A suite of characters in the latter matrix that were used to examine broader vombatiform relationships were excluded. With the addition of *W. schouteni* to the data matrix all taxa were rescored and characters revised resulting in the modification and addition of some characters.

The data matrix contained 64 morphological characters (21 cranial and 43 dental characters; see Supplemental material). Eighteen characters were considered transformation series and were ordered in the analysis. All characters were parsimony-informative. The late Oligocene–early Miocene peramelemorphian *Galadi speciosus* Travouillon *et al.*, 2010 and the early Miocene dasyurid *Barynya wangala* Wroe, 1999 were used as outgroups. The 10 thylacoleonid species were ingroup taxa. The dentary of *Thylacoleo* sp. cf. *T. hilli* (AM F63584) was used to score lower dentition characters for *T. hilli* because of the limited specimens of the latter, and because it is likely to be referable to that species. Characters of the humerus were not included because of the lack of these elements for most thylacoleonid species (seven of 10 taxa) and the two outgroups.

The matrix was analysed using maximum parsimony. A branch and bound heuristic search was used with characters equally weighted. The resulting most parsimonious trees were summarized using strict consensus. Bootstrap analysis was performed with 1000 replicates.

Body mass estimate

Estimates of the body mass of *Wakaleo schouteni* (QM F45200) were made using two regression equations from Myers (2001) and the total skull length variable (TSL = 164 mm). As recommended by Myers (2001), smearing estimates were applied to the values obtained. The first estimate was based on the regression equation from the ‘all species’ dataset ($\log y = -3.733 + 3.641[\log x]$) where x = total skull length (Myers 2001, table 2, p. 103). A smearing estimate of 5.5% was applied to the value obtained from this regression. The second estimate used the regression equation from the ‘diprotodontians’ dataset ($\log y = -3.410 + 3.508[\log x]$), where x = total skull length (Myers 2001, table 5, p. 106). A smearing estimate of 4.9% was applied to the resulting estimate.

Terminology

Terms relating to the fossil assemblages of the Riversleigh World Heritage Area (WHA) follow Arena *et al.* (2015) and Travouillon *et al.* (2011) and include the following: an individual faunal assemblage is referred to as a local fauna (LF); based on its faunal composition, each Riversleigh local fauna has been allocated to a biochronological unit or Faunal Zone (FZ). Four Faunal Zones are recognized at Riversleigh, each corresponding to a different time period: FZ A, late Oligocene; FZ B, early Miocene; FZ C, middle Miocene; FZ D, early–late Miocene.

Dental nomenclature follows Flower (1867) such that premolars are numbered P1–3 and molars are numbered M1–4. Superscript denotes upper teeth (e.g. upper first molar M^4); subscript denotes lower teeth (lower first molar M_1). Cranial terminology follows Aplin (1990). Basicranial terminology follows Archer (1976a).

Institutional abbreviations

AM F: Australian Museum Fossil Collection, Sydney, Australia; **CPC:** Commonwealth Palaeontological collection, Canberra, Australia; **FU, FO:** Flinders University Palaeontological collection, Adelaide, Australia; **NTM P:** Museums and Art Galleries of the Northern Territory, Palaeontological collection, Alice Springs, Australia; **QM F:** Queensland Museum, Fossil collection, Brisbane, Australia; **SAM P:** South Australian Museum, Palaeontological collection, Adelaide, Australia; **UCMP:** University of California, Berkeley, CA, USA, Palaeontological collection.

Systematic palaeontology

Class **Marsupialia** Illiger, 1811
 Order **Diprotodontia** Owen, 1866
 Suborder **Vombatiformes** Woodburne, 1984
 Family **Thylacoleonidae** Gill, 1872
 Genus **Wakaleo** Clemens & Plane, 1974

Type species. *Wakaleo oldfieldi* Clemens & Plane, 1974.

Included species. *Wakaleo vanderleuerei* Clemens & Plane, 1974; *Wakaleo alcootaensis* Archer & Rich, 1982; *Wakaleo schouteni* sp. nov.

Emended diagnosis. Species of *Wakaleo* are distinguished from those of *Thylacoleo* in the following combination of features: the cranium is mesocephalic rather than brachycephalic; upper molars are more triangular; all *Wakaleo* species except *W. alcootaensis* retain $M^{3/3}$; the P^3 and upper molars form a gently arcuate cheektooth row; $P^{3/3}$ is proportionately shorter relative to $M^{1/1}$. The P^3 of species of *Wakaleo* differ from species of *Thylacoleo* in having the following features: broader posteriorly than anteriorly with a prominent posterior cusp that is similar in height or slightly shorter than the anterior cusp; anterior and posterior cusps connected by a more arcuate (occlusal view) longitudinal blade; posterior longitudinal blade is concave in profile; a v-shaped valley extends between the anterior and posterior cusps on the lingual surface; a well-developed posterobuccal crest that extends buccally from the posterior end of the longitudinal blade and forms the posterior margin of a posterobuccal basin; a short and more prominent anterolingual crest that is cusplike (rather than a long vertical crest); a short buccal crest that extends anteriorly from the posterior cusp; a thicker and more linguallly-curved base of the anterior crest; and, posterolingual crest absent. Species of *Wakaleo* further differ from those of *Thylacoleo* in having: M^1 slightly longer than wide rather than being much longer than wide, and lacking a neoanterobuccal cusp (*sensu* Archer & Rich 1982); the C^1 alveolus much larger than the I^3 alveolus and situated anterior to P^1 rather than lingual to that tooth. The skull of species of *Wakaleo* differ from the skull of *Thylacoleo carnifex* in the following features: the frontal fails to contact the squamosal posteriorly; the tympanic wing consists of contributions from the alisphenoid and squamosal; the postglenoid process is relatively narrow and does not curve posteroventrally toward the mastoid process; a postorbital bar is absent; and, relative to total skull length, has a proportionally shorter frontal and proportionally longer parietal.

Species of *Wakaleo* differ from *Priscileo roskellyae* in the following combination of features: the cranium is larger and more robust, has a deeper and more rounded rostrum, and has tall, well-developed, sagittal and nuchal crests; the canine alveoli are relatively large, extending to

or beyond the anterior palatine foramen; presence of P^1 and P^2 is variable; the cheekteeth are more robust with more exposed roots, especially P^3 . M^1 and M^2 differ from those of *P. roskellyae* in having: metacone and paracone proportionately much taller and broader; protocone relatively more posteriorly situated; and, the crown below the protocone more bulbous; M^1 with a broader stylar basin anteriorly and narrower basin posteriorly, a stylar basin with a buccal edge which is lower than the paracone and metacone, and lacking a prominent buccal expansion of the crown adjacent to the paracone. M^2 also differs in being proportionately broader anteriorly; has a broader stylar shelf; a paracone which is more medially situated; postprotocristid that is posterobuccally orientated rather than posteriorly orientated; an anterior cingulum that does not extend to the protocone; it has a taller buccal margin relative to the protocone; the postparacrista and premetacrista meet relatively medially rather than near the buccal edge of the crown; has a steeper premetacrista; a trigon basin that is smaller relative to the width of the crown; and, has a steeper buccal face. Species of *Wakaleo* further differ from *P. roskellyae* in having: no more than two single-rooted teeth between I_1 and P_3 ; M_1 and M_2 with narrower and deeper talonid basins; M_1 talonid basin lacking posterolingual lengthening; the anterior basin of M_2 square (rather than triangular) and more medially situated.

The crania of species of *Wakaleo* also differ from that of *Priscileo roskellyae* in having: distinct palatal ridges; the dorsal surface of the neurocranium predominantly concave; the pterygoid fossa of the alisphenoid predominantly concave and pierced by a large transverse canal; the alisphenoid with lateral pterygoid processes; the postglenoid process lacks intrusion by the postglenoid cavity; a prominent rostral tympanic process (*sensu* Crosby & Norris 2003) on the periotic; the post-tympanic process of the squamosal extends across the entire anterior surface of the mastoid process rather than just the lateral portion of the anterior surface; the sulcus for the facial nerve (stylo-mastoid sulcus) passes through the post-tympanic process of the squamosal rather than through the mastoid; a relatively narrower outer ear canal; and, supraorbital processes that extend beyond the lateral edge of the infraorbital margin of the maxilla.

Species of *Wakaleo* differ from *Microleo attenboroughi* in: being much larger; having molars with more pronounced crenulations and roots that are more exposed; the P^2 alveolus being small relative to P^3 ; having P^3 narrower anteriorly than posteriorly and with a longitudinal blade that is buccally concave and lacking a medial cusplike and accessory anterobuccal cusplike; having the posterior longitudinal blade relatively horizontal rather than being steeply inclined and, consequently, a posterior end similar in height to the posterior cusp (rather than being much lower); having a shallower posterobuccal basin; having M^2 with a buccal margin that is taller than the lingual

margin, paracone taller than protocone, metaconule less pronounced, buccal expansion of the crown adjacent to the paracone, and lacking a notch on the lingual margin; lacking a pyramidal paracone on M^3 ; having M_3 less rectangular, lacking a rectangular talonid basin, and lacking a buccal and lingual midcrown groove.

Wakaleo schouteni sp. nov.
(Figs 2–7)

Diagnosis. *Wakaleo schouteni* differs from all other species of *Wakaleo* in: retaining four molars; having two teeth located between I_1 and P_3 ; having P_3 relatively similar in length to M_1 ; having M^1 with a squarer lingual margin; and in being smaller.

It also differs from *W. oldfieldi* and *W. vanderleuerei* in having: relatively broader talonid basins on M_{1-3} ; a relatively broader anterior basin on M_1 ; the entoconid and hypoconid on M_1 more widely separated; P_3 with a more sharply defined anterolingual crest and greater concavity between that crest and the anterior crest (rather than a broadly convex one).

Wakaleo schouteni further differs from *W. vanderleuerei* in having a cranium with the following distinctive features. The skull is relatively shorter and dorsally flatter. It has broad, dorsally depressed frontals that have raised and thickened supraorbital margins. It has relatively smaller and more anteriorly situated supraorbital processes. The occiput is relatively shorter and more rounded, lacks a medial septum and has deeper lateral fossae. The nuchal crest has a central posterior concavity. The postglenoid cavity lacks a horizontal septum. There is a narrower glenoid fossa, a broader postglenoid process and a more prominent medial glenoid process. The composite tympanic wing (with squamosal and alisphenoid components) is relatively flatter. There is a more obtuse rostral tympanic process on the petiote. The medial surface of the zygomatic arch is buttressed and lacks a masseteric process. In terms of differences in dental features, *W. schouteni* differs from *W. vanderleuerei* in not having the C^1 alveolus extend beyond the posterior margin of anterior palatine foramen. The M^2 has a larger metaconule and its crown has a relatively squarer outline. *Wakaleo schouteni* differs from *W. alcootaensis* in retaining P^1 and P^2 , and has a less arcuate molar tooth row.

Derivation of name. Named in honour of Peter Schouten for his exceptional reconstructions of Australia's prehistoric animals, and in particular those from the Riversleigh WHA.

Holotype. QM F45200, from Hiatus Site, a near-complete skull with transverse fracture in the region of postorbital constriction, with left $I^1 C^1 P^3 M^{1-3}$ and right $C^1 M^{1-4}$, and alveoli for left $I^{2-3} P^2$ and M^4 , and right $I^{1-3} P^{2-3}$.

Paratypes. From Rackham's Low Lion Site, QM F23443, a palate with left and right $C^1 P^3 M^{1-3}$ and alveoli for P^{1-2} and M^4 , an edentulous left dentary with the roots of $P_3 M_{1-2}$ and alveoli for $I_1 M_{3-4}$ and, a right distal humerus. From White Hunter Site, QM F52247, left and right dentaries, both with $P_3 M_{1-3}$ and alveoli for I_1, P_{1-2} , and M_4 ; QM F57904, a left humerus.

Referred material. From Bone Reef Site, QM F57314, a left maxillary fragment with alveoli for $P^3 M^{1-4}$; QM F57943, M_2 . From Burnt Offering Site, NTM P 91167-3, a right dentary with $P_3 M_{1-4}$; and NTM P91171-4, a P_3 . From D Site, QM F23446, a left maxillary fragment with broken P^1, P^3, M^{1-3} and alveoli for C^1 and P^2 ; QM F31439, a right I_1 . From Dirk's Towers Site, QM F24680, a left maxillary fragment with M^2 and alveoli for $P^3 M^{1-3-4}$; QM F30250, a left M^1 ; QM F30073, a left M_1 . From Hiatus Site, QM F57311, a right maxillary fragment with M^{1-2} , the posterior root of P^3 and alveoli for M^{3-4} ; QM F 57905, a left distal humerus; QM F57906, a right calcaneum. From Neville's Garden Site, QM F23801, a right M^2 . From Rackham's Low Lion Site, QM F52239, a left distal radius; QM F52238, a left proximal ulna; QM F52240, a left hamatum; QM F52241, a left trapezium; QM F52242, a left first metacarpal; QM F52243, a right proximal phalanx; QM F52244, a left proximal phalanx (pollex); QM F52245, a right medial phalanx; QM 52246, a left calcaneum; QM F52183, a cervical vertebra; QM F52185, a fifth lumbar vertebra; QM F52184, a sixth lumbar vertebra; QM F52186, a sacrum; QM F52187, left and right ilia. From Upper Site, QM F23441, a left M^1 ; and QM F23449, a left M_1 . From White Hunter Site, QM F30465, a left dentary with $I_1 P_3 M_{1-2}$ and alveoli for $P^2 M_{3-4}$; QM F31376, a left dentary with $I_1 P_3, M_{1-2}$; QM F57945, a right maxillary fragment with $P^3 M^{1-2}$ and alveoli for $C^1 P^{1-2} M^{3-4}$; QM F57944, a right M^1 .

Occurrence. The holotype is from Hiatus Site, Riversleigh WHA, Boodjamulla National Park, north-western Queensland. Locality co-ordinates for this site are held by Queensland Parks and Wildlife Service. Hiatus Site is regarded as being part of Riversleigh's Faunal Zone A which is interpreted to be late Oligocene in age (Archer *et al.* 1989, 1994, 1997; Arena 2004; Travouillon *et al.* 2006).

Bone Reef, Burnt Offering, D, Dirk's Towers, Neville's Garden, Rackham's Low Lion, Upper and White Hunter Sites are located within the Riversleigh WHA, Boodjamulla National Park, north-western Queensland. Bone Reef, Burnt Offering, D, Rackham's Low Lion, and White Hunter Sites are assigned to Riversleigh's Faunal Zone A which is interpreted to be late Oligocene in age (Archer *et al.* 1989, 1994, 1997; Arena 2004; Travouillon *et al.* 2006). Dirk's Towers, Neville's Garden and Upper Sites are part of Riversleigh's Faunal Zone B and are estimated to be early Miocene in age. Neville's Garden has been radiometrically dated at 18.24 ± 0.27 Ma and $17.85 \pm$

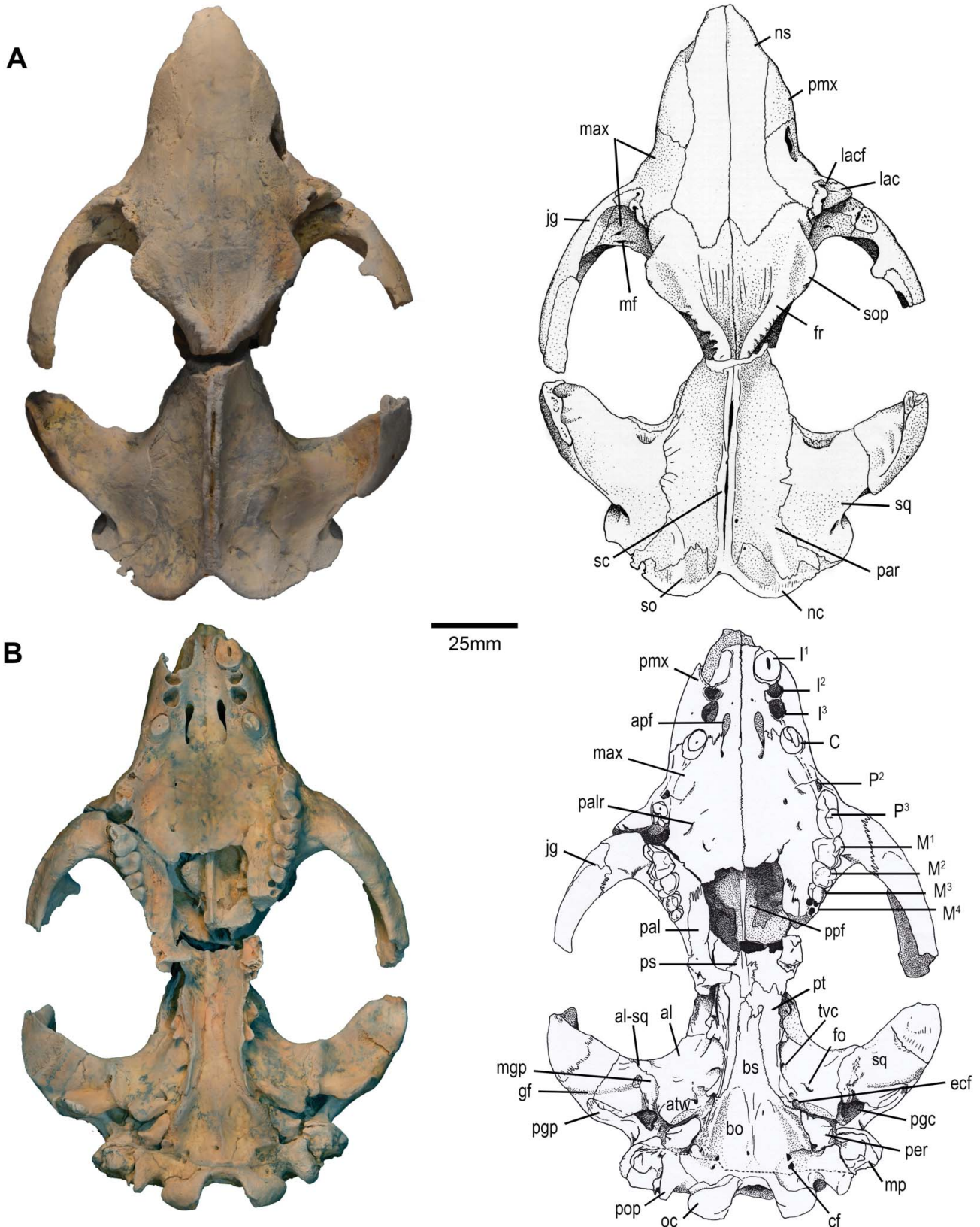


Figure 2. *Wakaleo schouteni* sp. nov. skull, QM F45200; **A**, dorsal view; **B**, ventral view. Abbreviations: al, alisphenoid; al-sq, alisphenoid squamosal suture; apf, anterior palatine foramen; atw, alisphenoid tympanic wing; bo, basioccipital; bs, basisphenoid; C, canine; cf, condyloid foramen; ecf, entocarotid foramen; fo, foramen ovale; fr, frontal; gf, glenoid fossa; I, incisor; jg, jugal; lac, lacrimal; lacf, lacrimal foramen; M, molar; max, maxilla; mf, maxillary foramen; mgp, medial glenoid process; mp, mastoid process; nc, nuchal crest; ns, nasal; oc, occipital condyle; P, premolar; pal, palatine; palr, palatine ridge; par, parietal; per, periotic; pgc, postglenoid cavity; pgp, postglenoid process; pmx, premaxilla; pop, paroccipital process; ppf, posterior palatal fenestra; ps, presphenoid; pt, pterygoid; sc, sagittal crest; so, supraoccipital; sop, supraorbital process; sq, squamosal; tvc, transverse canal.

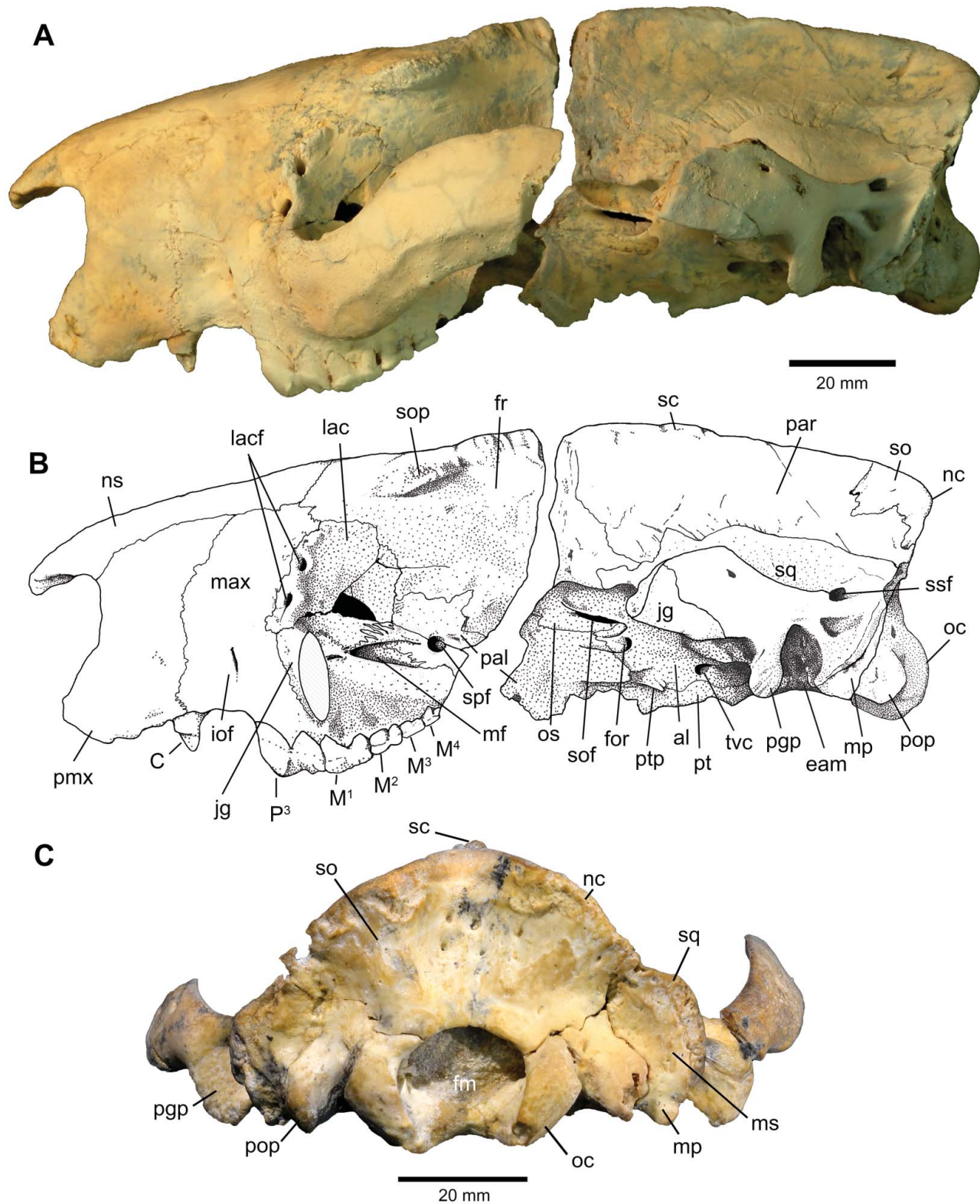


Figure 3. *Wakaleo schouteni* sp. nov. skull, QM F45200; **A**, left lateral view; **B**, left lateral view with jugal removed (hatched area) and M⁴ included; **C**, posterior view. Abbreviations: al, alisphenoid; C, canine; eam, external auditory meatus; fm, foramen magnum; for, foramen rotundum; fr, frontal; iof, infraorbital foramen; jg, jugal; lac, lacrimal; lacf, lacrimal foramen; M, molar; max, maxilla; mf, maxillary foramen; mp, mastoid process; ms, mastoid; nc, nuchal crest; ns, nasal; oc, occipital condyle; os, orbitosphenoid; P, premolar; pal, palatine; par, parietal; pgp, postglenoid process; pmx, premaxilla; pop, paroccipital process; pt, pterygoid; ptp, pterygoid process of the alisphenoid; sc, sagittal crest; so, supraoccipital; sof, sphenorbital fissure; sop, supraorbital process; spf, sphenopalatine foramen; sq, squamosal; ssf, subsquamosal fossa; tv, transverse canal.

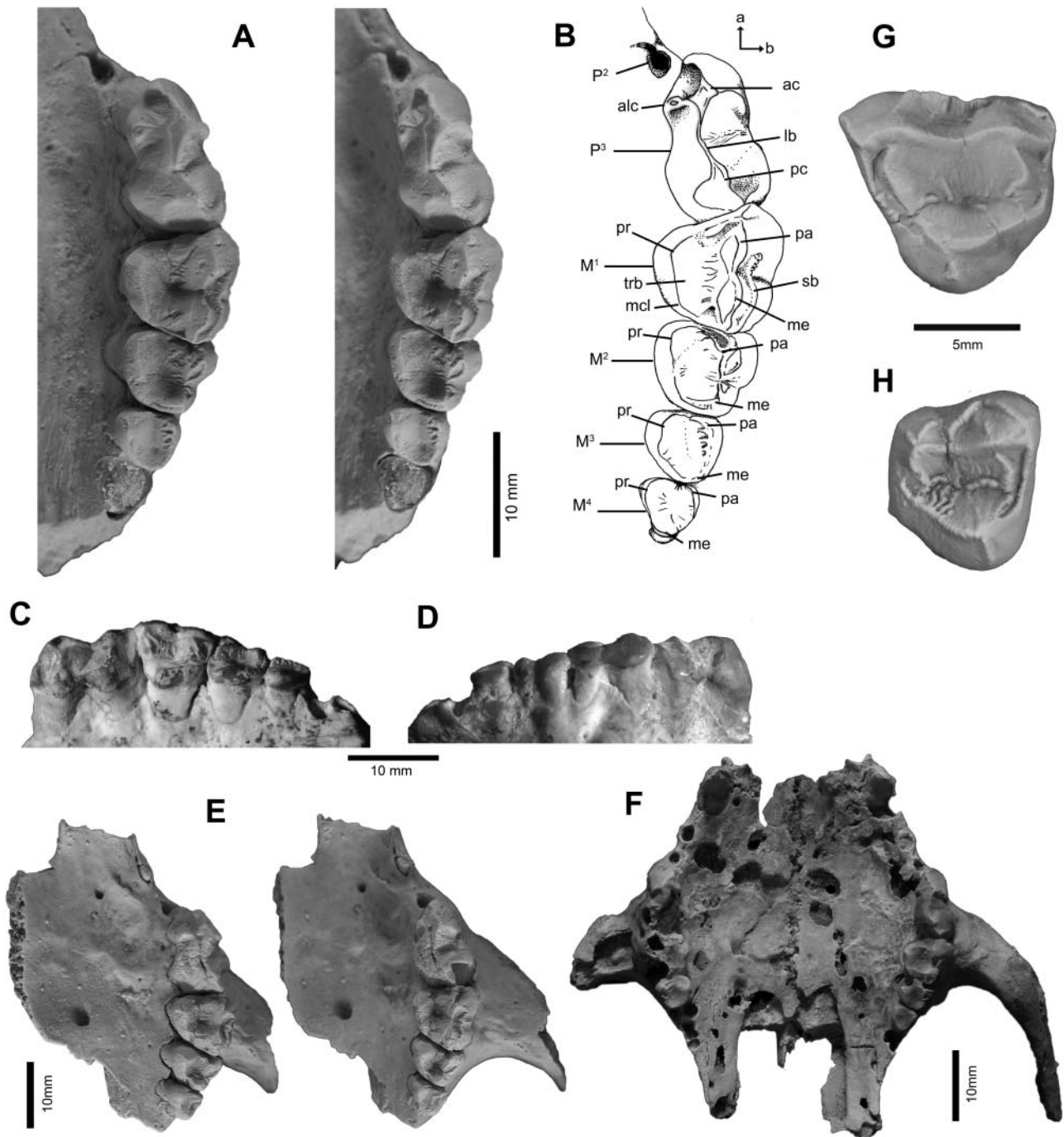


Figure 5. Upper dentitions of *Wakaleo schouteni* sp. nov. **A–D**, QM F45200, holotype, upper left P^3 , M^{1-4} (M^4 is a superimposed mirror image from the right side); **A**, stereophotographs of upper left cheektooth row; **B**, interpretive drawing of the same; **C**, lingual view of left cheektooth row; **D**, buccal view of left cheektooth row. **E**, QM F23446, stereo photographs of a left maxillary fragment from D Site with $P^{1,3}$, M^{1-3} . **F**, QM F23443, palate from Rackham's Low Lion Site. **G**, QM F30250, left M^1 from Dirk's Towers Site. **H**, QM F23801, right M^2 from Neville's Garden Site. Abbreviations: ac, anterior cusp; alc, anterolingual cusp; lb, longitudinal blade, M, molar; me, metacone; mcl, metaconule; P, premolar; pa, paracone; pr, protocone; sb, stylar basin; trb, trigon basin.

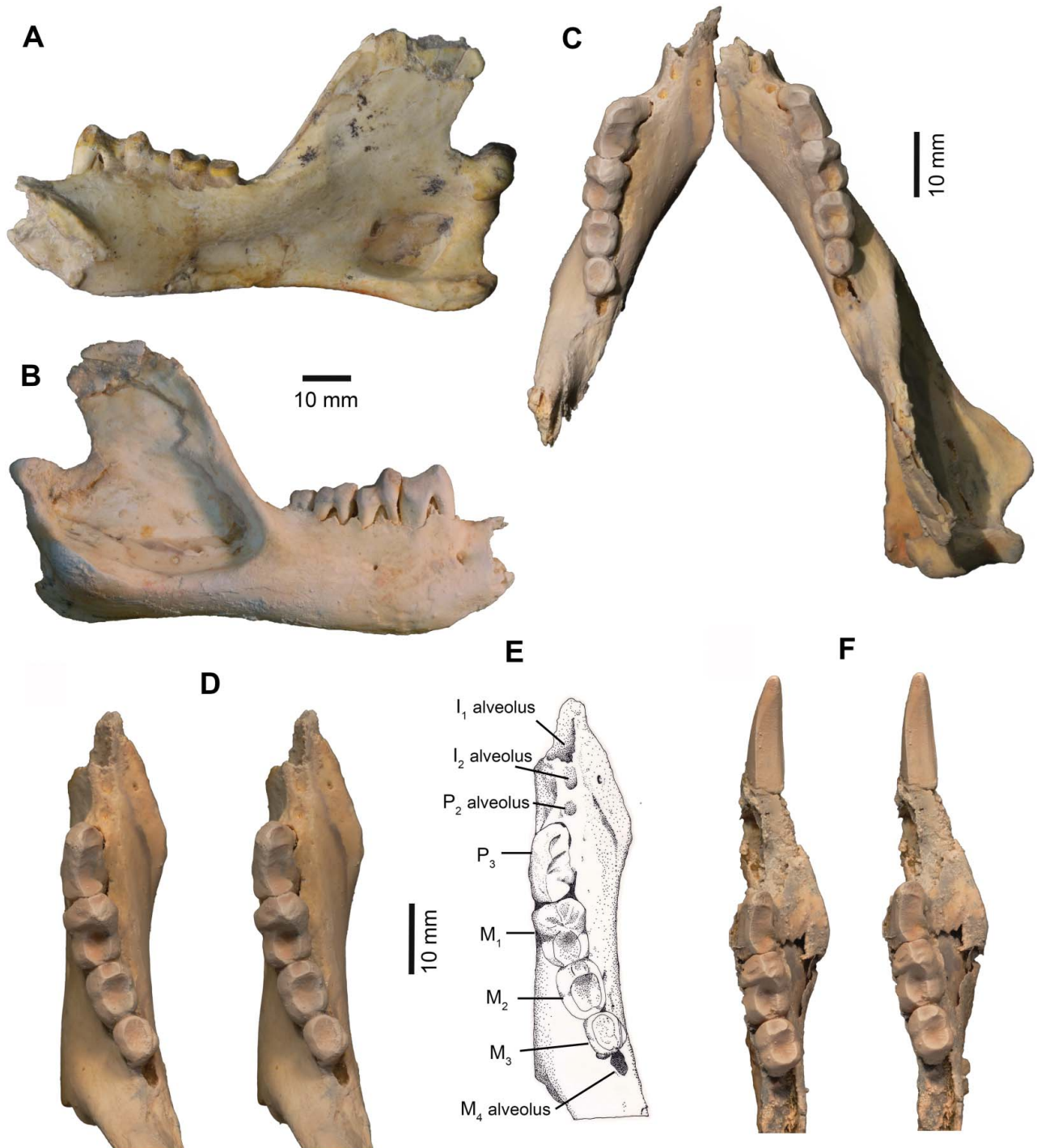


Figure 6. Mandibles of *Wakaleo schouteni* sp. nov. **A–E**, QM F52247; right dentary with P₃, M₁₋₃; **A**, lingual view; **B**, buccal view; **C**, occlusal view of left and right dentaries; **D**, occlusal view, stereo pair of left dentary; **E**, interpretive drawing of left dentary. **F**, QM F31376, occlusal view, stereo pair of left dentary, I₁, P₃, M₁₋₃. Scale bar = 10 mm.

rounded laterally and anteriorly, and in profile, has a more inclined dorsal margin.

Nasal. The nasals are long (71.0 mm) and narrow. In dorsal view they are narrow anteriorly, become wider at

the level of the posterior edge of the narial opening, and together form a triangular, convex roof over this opening (Fig. 2A). Posteriorly, the nasals widen again at the level of the superior lacrimal foramen and then narrow again to form a deep M-shaped contact with the frontals. The

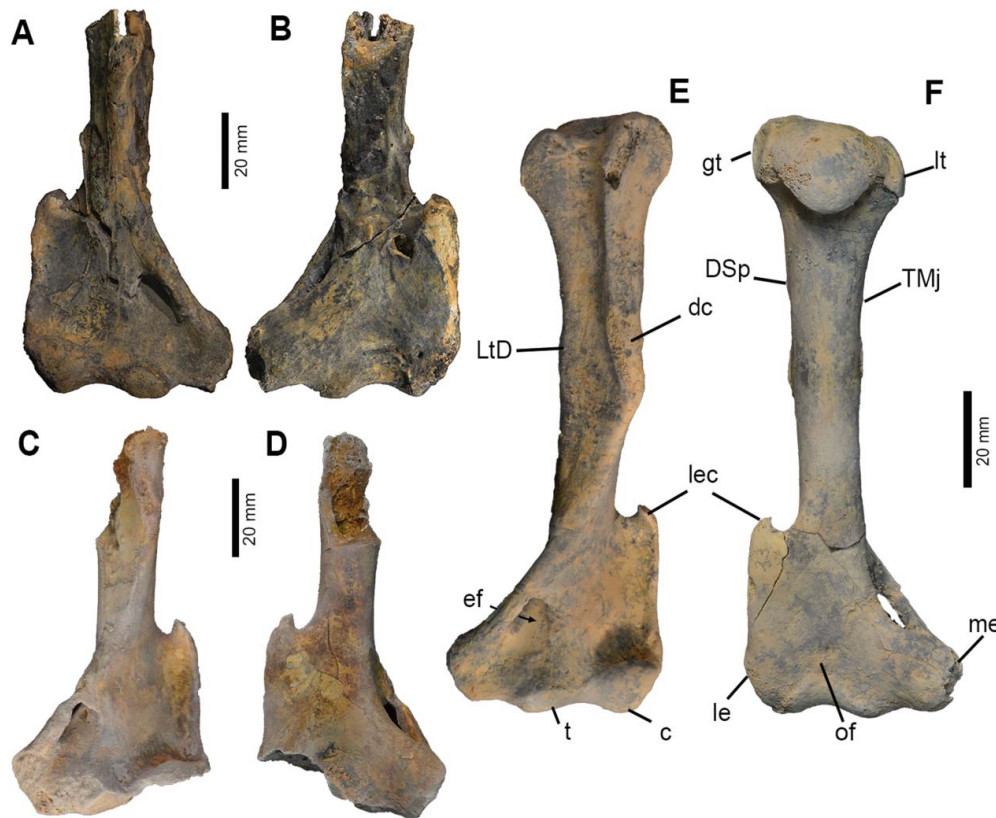


Figure 7. Humeri of *Wakaleo schouteni* sp. nov. **A, B**, QM F23443; **A**, anterior view; **B**, posterior view. **C, D**, QM F57905; **C**, anterior view; **D**, posterior view. **E, F**, QM F57904; **E**, anterior view; **F**, posterior view. Abbreviations: c, capitulum; dc, deltoid crest; DSp, deltoid pars spinalis tubercle; ef, entepicondylar foramen; gt, greater tubercle; LtD, latissimus dorsi rugosity; le, lateral epicondyle; lec, lateral epicondylar crest; lt, lesser tubercle; me, medial epicondyle; of, olecranon fossa; t, trochanter; TMj, teres major tubercle.

Table 1. Measurements of cranial dimensions (in mm) of *Wakaleo schouteni* sp. nov. and *Wakaleo vanderleueri*.

		Skull length	Skull depth	Occiput width	Occiput depth	Supraorbital width	Zygomatic width
<i>W. schouteni</i>	QM F45200	164.0	[63]	73.2	27.7	47.1	111.8
<i>W. vanderleueri</i>	CPC 26604	186.8	79.3	73.4	34.5	66.4	[135]

[] = approximate; skull length = tip of nasals to nuchal crest; skull depth = height between dorsum of skull and the occlusal surface at P3/M1; occiput width = breadth of occiput between lateral edges of squamosal; occiput depth = nuchal crest to dorsal margin of foramen magnum.

lateral margins of the nasals are rounded and form a gently arched contact with the premaxilla and maxilla (Fig. 3A, B). In *W. vanderleueri* the lateral margins are more markedly rounded and the nasals are slightly pinched near their midpoint. Dorsal to the narial opening the nasals are distinctly convex, unlike in *W. vanderleueri* and *P. roskellyae* in which they are flatter, especially in the latter. Posteriorly, the nasals are slightly inflated but less so than in *P. roskellyae* and they are unlike those in *W. vanderleueri* which form a slight depression.

Premaxilla. In frontal view, the premaxillae are gently convex; together with the nasals they form a heart-shaped nasal aperture which is broader (26 mm) than high

(18.7 mm). In profile, the premaxillae are taller than long (Fig. 3A, B) and are similarly proportioned to those in *W. vanderleueri*. In *P. roskellyae* the premaxillae are relatively dorsoventrally shorter. The nasopremaxillary suture is slightly arched, rising posteriorly. The premaxilla contacts the maxilla at the canine alveolus. This suture extends dorsally from the midpoint of the canine alveolus and curves posteriorly as it approaches the nasal. In *W. vanderleueri* and *P. roskellyae* this suture courses more vertically as it nears the nasals.

Ventrally, the premaxilla bears alveoli for three incisors. The size relationship of the sockets is $I^1 > I^2 < I^3$ (Fig. 2B). This condition is found in all thylacoleonids except *Microleo attenboroughi* for which the condition is

unknown. The I^1 alveolus is large and longitudinally elliptical. It extends posteriorly above the alveoli of I^2 and I^3 . The alveolus for I^2 occurs immediately posterior to I^1 and is slightly anteroposteriorly compressed. It is much shorter than that for I^1 . The I^3 alveolus occurs immediately posterior to I^2 , is round and relatively shallow. The premaxilla extends for 2.5 mm posterior to the I^3 alveolus where it forms the anterior wall of the canine alveolus.

A narrow palatal arch is present within the narrow U-shaped incisor arcade. This arch is proportionally similar to that of *W. vanderleueri* and relatively narrower than that of *P. roskellyae*. Elongate anterior palatal foramina (11 mm long, 2.5 mm wide) occur medial to I^3 and the canine and extend posteriorly to just beyond the canines. In *W. vanderleueri* these foramina extend to the posterior third of the canine and in *P. roskellyae* they extend well beyond the canine. In *W. schouteni* the lateral margins of the foramen are on a more ventral level than their medial margins which are formed by the medial palatal processes of the premaxillae. Together, these processes form a 6.5 mm wide bridge anteriorly. Posteriorly, they narrow and result in a widening of the foramina. The premaxillo-maxillary suture courses transversely between the medial edge of the canine alveolus and the lateral margin of the foramen.

Maxilla. In lateral view, the maxilla anterior to the orbit is roughly rectangular in outline and is taller than it is broad (Fig. 3A, B). Its length is similar to that of the premaxilla and it is relatively longer than the maxilla of *W. vanderleueri* but shorter than that of *P. roskellyae*. Dorsally it forms a short (14.6 mm) arched contact with the nasal. Posterodorsally it contacts the anterolateral edge of the frontal. Similar sutural relations are seen in *W. vanderleueri* and *P. roskellyae*. The maxilla is laterally convex. A large infraorbital foramen is situated in the lower third about midway between the premaxilla and the suture with the jugal. This foramen is subtriangular and anteriorly directed. The zygomatic process of the maxilla extends laterally at an angle of 70° with the median plane and forms a broad anterior margin of the orbit as in *W. vanderleueri*. However, it differs from that species in having a slightly thinner process that lacks anterodorsal thickening at the anterior of the orbit and lacks a masseteric process on its ventral surface. *Priscileo roskellyae* has a much thinner and less robust zygomatic process and also lacks a masseteric process. The maxillojugal suture is inclined relatively steeply and differs from *W. vanderleueri* which has a more oblique suture that results from the anterior portion of the jugal extending anterodorsally towards the anterior margin of the lacrimal foramen.

The maxilla forms a deep suborbital shelf at the anteroventral margin of the orbit. At the medial margin of the shelf the maxilla contacts the lacrimal. The maxillolacrima suture courses posteroventrally from the anterior edge

of the orbit, just posterior to the inferior lacrimal foramen, to a large maxillary foramen which occurs near the midpoint of the medial margin. The maxillary foramen opens posteriorly into deep sulcus. At this foramen the maxilla contacts the palatine; the maxillopalatine suture courses posteriorly along the medial wall of the sulcus and descends to the palatal surface 10 mm posterior to M^4 . Lateral to the maxillary foramen the maxilla bears a number of deep horizontal grooves and numerous alveolar foramina.

The maxilla bears the posterior half of the canine alveolus, one or two single-rooted anterior premolars, a double-rooted third premolar and four molars that progressively decrease in size (Fig. 2B). P^3 is deflected medially relative to the molar row and the angle it forms is similar to that in *W. vanderleueri* whereas in *P. roskellyae* the degree of deflection is much smaller. The maxillary palate is generally broad and rhomboid-like in shape and similar to that of *W. vanderleueri* and *P. roskellyae* (Fig. 2B). From the front of the palatal arch to the anterior margin of the posterior palatal fenestrae the palate measures 60.0 mm. The palate is widest (41.6 mm) just posterior to P^3 . The palatal arch is gently concave in the region of the premaxillo-maxillary suture and increases its curvature at the level of P^3 . Two short (4–5 mm) palatal ridges lie at the lateral margins; one lies medial to the C^1 – P^2 diastema and a second ridge lies medial to the posterior root of P^3 . Both ridges are anteromedially orientated. Similar ridges are present in *W. vanderleueri* but are absent in *P. roskellyae*. Large nutrient foramina lie medial to P^2/P^3 and M^1/M^2 . Similar foramina are found in *W. vanderleueri* and *P. roskellyae*. Numerous pinhole-sized foramina occur just medial to the roots of the molars. Large posterior palatal fenestrae (21.0 mm wide, 28.5 mm long) extend from the level of M^1/M^2 to the transverse palatine process. The fenestrae are proportionally larger than those of *W. vanderleueri* but smaller than those of *P. roskellyae*. Although missing in QM F45200, in QM F23443 a small spinous process of the maxilla extends posteriorly into the fenestrae at the region of intermaxillary suture. As in *W. vanderleueri*, the fenestrae are posteriorly enclosed by a transverse palatine process, of which only a portion is preserved near the posterior end of the right post-alveolar process. The highly convoluted maxillopalatine suture courses posterolaterally from the lateral margin of the posterior palatal fenestra (at approximately the level of M^2) to the lateral margin of the postalveolar process, approximately 9 mm posterior to the M^4 alveolus.

Jugal. The jugal is only partially preserved. It is thick and extends posterolaterally, contributing to a broad, robust face. It forms the anterolateral margin of the orbit and anteriorly makes a steep, oblique contact with the maxilla and contacts the lacrimal at its mediodorsal extremity (Fig. 3A). The anterior depth of the jugal is less

than in *W. vanderleuerei* which is much deeper lateral to the masseteric process. From its anterior border with the maxilla, the jugal curves dorsally and has a concave dorsal edge on the anterior half of the zygomatic arch. The jugal contacts the squamosal on the dorsal edge of the zygomatic arch 22.1 mm posterior to its contact with the lacrimal. The jugal extends posteriorly below the squamosal and becomes dorsoventrally thinner and wider at its posterior extremity. A distinct ridge, the masseteric border, occurs along the ventral third of its lateral surface. The jugal surface ventral to this border is medially orientated. The jugal terminates 8.3 mm anterolateral to the glenoid process.

Frontal. In dorsal view, the frontals are broad anteriorly and strongly constricted posteriorly (Fig. 2A). Anteriorly, the paired bones form a deep w-shaped contact with the nasals anteriorly and with the maxilla anterolaterally. The frontals form distinct triangular supraorbital processes that project laterally into the orbit (Fig. 2A). The processes are rugose and thick (5.2 mm). The width between the supraorbital processes is 47.1 mm. In between these two processes the frontals form a broad fossa that narrows posteriorly. *Priscileo roskellyae* also exhibits a dorsal fossa of the frontals and supraorbital processes, although the processes in that species are much thinner. The anterior surface of the fossa bears many longitudinal striations and the posterior surface is covered by numerous small pits. The posteriorly converging lateral margins of the fossa are raised and thickened (5.1 mm) and commence anteriorly as slight ridges on the supraorbital processes and become more prominent as they converge (Figs 2A, 3A, B). The dorsum of the skull of *W. vanderleuerei* differs markedly in having distinct dorsally rounded frontals that extend posteriad well beyond the postorbital constriction and contribute to the anterior part of the cranial roof. Its supraorbital processes are also larger and thicker, and are more posteriorly situated at approximately the midpoint of the orbital fossa.

Lacrimal. The lacrimal forms the anteromedial wall of the orbit and extends anteriorly onto the face for a short distance (Figs 2A, 3A, B). A narrow tongue of the lacrimal also extends laterally along the anterodorsal margin of the orbit. The lacrimal is similar in shape to that bone in *W. vanderleuerei* and *P. roskellyae*; however, the anterior excursion onto the face in the latter is minimal. Two foramina occur in the facial portion of the lacrimal, one above the other. The superior foramen occurs in a raised and extremely rugose area at the anteromedial edge of orbit. In *W. vanderleuerei* the area around the foramen is only minimally raised and lacks rugosity. The superior foramen is small (2.3 mm wide) and dorsally directed. The inferior foramen is situated on the rostrum in a laterally directed fossa that is anterior and ventral to the superior foramen. It is larger and vertically elliptical. This

fossa in *W. vanderleuerei* is relatively larger and more triangular. The maxillo-lacrimal suture which is anterior to these foramina is highly convoluted. Dorsally, the suture arches posteriad, contacting the frontals, and then descends in a posteroventral direction across the medial wall of the orbit. Posteroventrally the lacrimal contacts the palatine just dorsal to the maxillary foramen.

Palatine. The transverse fracture of the skull passes through the palatines and thus they are incomplete. The palatine has a perpendicular process that contributes to the ventral half of the medial wall of the orbit and a horizontal process that forms the lateral and posterior margins of the posterior palatal fenestra (Figs 2B, 3A, B). The perpendicular process is approximately circular with a small anterior and a longer posterior projection. The anterior projection forms the medial wall of the maxillary foramen and is bordered dorsally by the lacrimal and ventrally by the maxilla. Posterior to this foramen the palatine enlarges to form a disc that is bordered dorsally by the frontal. The centre of this disc is pierced by a large (3 mm wide), round, anteromedially orientated sphenopalatine foramen. The posterior projection of the palatine extends into the sphenorbital fissure and is bordered posterodorsally by the orbitosphenoid, posteriorly by the alisphenoid and posterolaterally by the pterygoid. At its posterolateral border with the alisphenoid, lateral to the foramen rotundum, the palatine forms a small posterolaterally orientated process. On the palatal surface it forms the lateral margins of the posterior palatal fenestrae (Fig. 2B). It extends posteriorly from the level of M²⁻³ and at its posterior extremity forms a transverse palatine process (approx. 14.5 mm posterior to M⁴). Only the lateral margins of this process are preserved in QM F45200. Small, minor palatine foramina occur just anterior to the transverse palatine processes. The palatine of *W. vanderleuerei* is similar in form although it is figured in Murray *et al.* (1987, fig. 5B) as being incised by a small projection of the maxilla dorsal to the sphenorbital foramen. The sole cranial specimen of *W. vanderleuerei* bears numerous fractures that make difficult the identification of sutures and it is likely that the portion of bone marked as maxilla is part of the palatine. The palatine of *P. roskellyae* lacks the anterior height seen in *W. schouteni* and *W. vanderleuerei*.

Vomer. The nasopharyngeal canals are partly filled with matrix. A small segment of the sagittal part of the vomer is exposed at the anterior margin of the posterior palatal fenestrae. This part of the vomer forms a rounded septum and a relatively steep medial wall of the nasopharyngeal meatus. Posteriorly, its articulation with the pre-sphenoid and palatine is obscured.

Neurocranium. The neurocranium is anteriorly narrow and posteriorly broad (Fig. 2A). Relatively tall sagittal and nuchal crests are distinctive features on the dorsal

surface (Fig. 3A–C). Ventrally, the tympanic region is open. The tympanic wing is moderate in size. The outer ear canal is broad, affording a relatively unimpeded view of this region. The frontals, ethmoid, parietals and presphenoid are incomplete.

The neurocranium shares many similarities with that of *W. vanderleueri*, including tall sagittal and nuchal crests that descend steeply onto the temporal fossae and parietals that are predominantly concave but convex at their lateral extremity. In contrast, the sagittal and nuchal crests in *P. roskellyae* are relatively smaller. The occipital region is similar in absolute width to *W. vanderleueri* but is not as tall (Table 1).

Ethmoid. The posterior surface of the cribriform plate is exposed on the anterior half of the skull. The plate is 14.7 mm wide and is divided by a vertical septum. The surface of the plate is pierced by numerous foramina. Dorsally, the cribriform plate contacts the inner table of the frontal bone, a dense area of frontal bone that is also perforated with numerous small foramina.

Parietal. The parietals are long and relatively narrow (Fig. 2A). Anteriorly, their articulation with the frontals is obscured because of damage associated with the transverse fracture. Dorsally they form a tall, thickened ridge that together forms a strong sagittal crest. Below the sagittal crest the parietal laminae curve concavely and extend laterally to meet the squamosal (Fig. 3A, B). The dorsal edges of the squamosal laminae are missing (approx. 5 mm) and the underlying parietal surface bears many vertical grooves. At the posterior end of the sagittal crest the parietals do not ascend onto the nuchal crest but form a posteriorly concave margin with the squamous part of the supraoccipital bone, approximately 10 mm anterior to the nuchal crest (Figs 2A, 3A, B). The parietals extend to the nuchal crest at their posterolateral extremity. The parietals of *W. vanderleueri* are similar but anteriorly they flare laterally as they contact the inflated posterior region of the frontals, and posteriorly extend to the nuchal crest in their entirety. In contrast, the parietals of *P. roskellyae* are proportionately broader, predominantly convex and form a much smaller sagittal crest.

Orbitosphenoid. The orbitosphenoid is incomplete. In lateral view it forms the roof and the anterior floor of the sphenorbital fissure (Fig. 3A, B). It is bordered anterolaterally by the palatine, dorsally by the frontal, posteriorly by the basisphenoid and posterolaterally by the alisphenoid. The sphenorbital fissure is elongate (approx. 9 mm long) and deep. Dorsal to the fissure, the orbitosphenoid forms the anterior half of a broad and deep fossa which is delineated superiorly by a prominent infratemporal crest and inferiorly by a thin, sharp, horizontal crest (the alisphenoid forms the posterior part of this fossa).

Presphenoid. Ventrally, anterior to the basisphenoid, the presphenoid forms a narrow tongue of bone that is flanked by the palatines (Fig. 2B). Along its midline it forms a longitudinal septum which becomes narrower and more prominent anteriorly. At its lateral margins it forms a highly convoluted suture with the palatine.

Basisphenoid. The basisphenoid is roughly triangular, flat and inclined anterodorsally. It is narrow anteriorly where it contacts the presphenoid, broad posteriorly where it is strongly fused to the basioccipital, and is flanked by the pterygoids (Fig. 2B).

Pterygoid. Only the basal attachments of the pterygoid to the basisphenoid and alisphenoid are preserved. More of the left side (34.4 mm long) is preserved than the right. In ventral view, they extend from the posterior margin of the palatine to the opening for the internal carotid artery, curving laterally where they contact the basisphenoid (Fig. 2B).

Alisphenoid. The alisphenoid forms much of the anteroventral floor of the braincase. In lateral view, its dorsal contacts (from anterior to posterior) are the frontal, parietal and the squamosal. It forms the posterior edge of the infratemporal crest (Fig. 3A, B). Laterally, this crest becomes contiguous with the anterior edge of the zygomatic process. In this region the alisphenoid forms a small dorsal strip along the anterior edge of the zygomatic process and posteriorly makes a broad contact with the squamosal. Ventral to the infratemporal crest the alisphenoid forms a broad and deep infratemporal fossa, the ventral margin of which is formed by the sphenorbital fissure (Fig. 3A, B). The presphenoid forms the anterior part of this fossa and forms a sinuous vertical suture with the alisphenoid. A large, round foramen rotundum (3.0 mm wide) occurs at the posterior margin of the sphenorbital fissure. Lateral to the foramen rotundum the alisphenoid forms two flattened, laterally projecting processes; the posterior process is slightly ventral to and smaller than the anterior (lateral pterygoid process of the alisphenoid; Fig. 4A). In *W. vanderleueri* the anterior process is similarly developed but the posterior process is smaller than the process in *W. schouteni*. These processes are absent in *P. roskellyae*. Ventral to this process the alisphenoid contacts the pterygoid bone. Posterior to this process the alisphenoid forms a shallow, oval, pterygoid fossa that posteriorly bears the large, posterolaterally directed foramen of the transverse canal. The fossa and transverse canal in *W. vanderleueri* are similarly formed. The pterygoid fossa in *P. roskellyae* is distinctly different, being flattened anteriorly, slightly convex posteriorly and has a very small transverse canal.

In ventral view, the alisphenoid projects laterally from the pterygoid fossa to the medial base of the medial glenoid process as a broad, ventrally concave surface

(Figs 2B, 4A). At the base of the medial glenoid process it makes a sinuous contact with the squamosal. The opening of the internal carotid canal occurs approximately 10 mm posterior to the transverse canal. A broad sulcus extends posterolaterally from the carotid foramen and posteriorly the sulcus is overlain by the anterior end of the periotic. Posterolateral to the foramen of the transverse canal is the anteriorly orientated foramen ovale (3.5 mm wide). Posterior to the foramen ovale the alisphenoid forms a triangular tympanic wing (8–9 mm in width) and is the major element that floors the hypotympanic sinus. The alisphenoid tympanic wing is rounded posteriorly, ventrally convex, and contacts the squamosal at its anterior, medial and lateral margins. A distinct suture with this element can be seen on the anterior wall of the squamosal hypotympanic sinus (Figs 2B, 4B). The contribution of the alisphenoid to the tympanic floor varies between the left and right sides; on the right, the floor is formed completely by this element, on the left, the squamosal forms a small contribution at the anterolateral margin. The alisphenoid tympanic wing of *W. schouteni* differs from that of *W. vanderleuerei* in being flatter and shorter, and has a much greater distance separating it from the medial edge of the mastoid process.

Squamosal. In lateral view, the squamosal forms a convex wall over the lower two-thirds of the brain case and extends laterally to form a broad zygomatic process (Figs 2A, 3A, B). It is bordered dorsally by the parietal. On the left side much of the dorsal edge (5 mm) is missing although evidence of its contact is marked by the presence of numerous fine vertical grooves on the surface of the parietal. Anteriorly, it contacts the alisphenoid, but does not make contact with the frontal. Just dorsal to the anterior margin of the zygomatic process there is a small oval, medially inclined fossa. This fossa is also present in *W. vanderleuerei* but is absent in *P. roskellyae*. As the zygomatic process curves anteriorly its lateral edge rises to form a tall, thin margin that tilts medially to slightly overhang the orbit. The medial surface of the zygomatic process bears two buttress-like vertical ridges. The lateral surface is pierced by a foramen approximately 10 mm anterior to the glenoid notch.

In ventral view, the squamosal is bordered by the alisphenoid medially and the mastoid posteriorly (Figs 2B, 4A). The ventral surface of the zygomatic wing bears a transverse, deeply grooved glenoid fossa (14.5 mm wide). The fossa extends to the lateral edge of the zygoma. On the right zygomatic wing, anterolateral to the glenoid notch, the rugose, concave articular surface for the jugal is exposed. Posterior to the glenoid fossa the squamosal forms a broad (14 mm), deep (11.5 mm), rounded postglenoid process (Fig. 4A). This process in *W. vanderleuerei* is relatively narrower. At the medial margin of the fossa the squamosal forms a rugose ridge, the medial glenoid

process. This process is relatively larger than in *W. vanderleuerei*. It is posteromedially orientated from the orbital margin to the tympanic cavity, where it projects as a small process just lateral to the tympanic wing. The squamosal contacts the alisphenoid on the medial side of the medial glenoid process.

The squamosal is the main contributor to the roof of the auditory region. Medial to the posterior end of the medial glenoid process the squamosal extends anteriorly to form a squamosal hypotympanic sinus. In ventral view the sinus is roofed by the alisphenoid tympanic wing. The squamosal contacts the alisphenoid at the anteroventral margin of the hypotympanic sinus (Fig. 4B) such that if the alisphenoid tympanic wing were broken at its base it would appear as a bilaminar structure. *Wakaleo vanderleuerei* also has a bilaminar tympanic wing with an anterior squamosal contribution. However, any lateral contribution from this element cannot be determined in the sole cranial specimen of this species.

The posterior surface of the postglenoid process is broad and gently convex (Figs 3C, 4A) as is the condition in *W. vanderleuerei*. In contrast, in *Priscileo roskellyae* the posterior surface is invaded by the postglenoid cavity. Dorsal to this process the squamosal thickens to form a bridge between the posterior margin of the zygomatic process and the brain case. This bridge forms the roof of the external auditory meatus. At the posterior edge of the meatus the squamosal forms a ventral process, the post-tympanic process, which abuts the anterior surface of the mastoid. This process bears a deep, laterally directed stylo-mastoid sulcus. In contrast, the stylo-mastoid sulcus in *P. roskellyae* courses through the mastoid. A large (3.4 mm wide), oval, posteriorly orientated, subsquamosal foramen is situated on the posterolateral surface of the zygomatic process (Fig. 3A, B). A small triangular depression occurs ventral to this foramen at the posterodorsal edge of the external auditory meatus. Posterior to the subsquamosal foramen a narrow strip of the squamosal forms the lateral margin of the nuchal crest and abuts the posterior edge of the mastoid process (Fig. 3C). Medial to the postglenoid process the squamosal extends anterodorsally to form a deeply recessed postglenoid cavity.

Basioccipital. The basioccipital resembles that of *W. vanderleuerei*. It is more or less hexagonal and bears a central longitudinal crest that is low anteriorly and higher posteriorly (Fig. 2B). The central crest is flanked by broad, deep fossae. The lateral margins of the basioccipital that are medial to the entocarotid foramen and the periotic are raised, thickened and rugose. A large foramen pierces the basioccipital posteriorly near the central crest and a smaller foramen occurs anteriorly in the left fossa. A pair of moderately large foramina (opening for rami of the hypoglossal nerve) occurs at the posterolateral

margins of the basisphenoid. Both foramina lie in a small depression and are directed anteroventrally.

Occipital region. The occipital region is broad (73.2 mm wide) and deep (45.0 mm from the nuchal crest to the base of the occipital condyles; Fig. 3C). Its dorsal margin is strongly arched and formed by a prominent overhanging nuchal crest. As the lateral edges of the nuchal crest ascend toward the apex of the occiput they course anteriorly and form a broad recess in the centre of the crest (Fig. 2A). This recess is also present in *W. vanderleuerei* but is shallower. It is absent in *P. roskellyae*.

In posterior view the occipital surface is composed of three fossae; one central and two lateral (Fig. 3C). The supraoccipital is lens-shaped and bears the deep central fossa. In dorsal view, the squamous part of the supraoccipital is evident on the anterior surface of the nuchal crest where it forms a small fossa on each side of the sagittal crest. At its lateral margins the supraoccipital is bordered by the mastoid dorsally and exoccipital ventrally. The supraoccipito–exoccipital and supraoccipito–mastoid sutures course in a dorsolateral direction from just dorsal of the occipital condyles to the nuchal crest. The central fossa is similar to that of *W. vanderleuerei* in that it has a very weak central crest, numerous pinhole foramina and a number of larger foramina. In contrast, the central crest in *P. roskellyae* is more prominent and more rounded. The dorsolateral margins of the fossa are rugose. The central fossa is separated from the lateral fossae by broad, gently rounded crests that extend ventromedial from the nuchal crest toward the foramen magnum. The lateral fossae occur where the supraoccipito–exoccipital suture meets the supraoccipito–mastoid suture. These fossae are deeper than those in *W. vanderleuerei* and *P. roskellyae*.

The occipital condyles are large and prominent, and project posteriorly beyond the level of the nuchal crest (Fig. 3C). The condyles are rounded posteriorly and ventrally, and are separated by an 11.7 mm wide intercondyloid notch. The foramen magnum is large (12.0 mm high, 19.1 mm wide), oval and opens posteriorly. A pair of foramina is situated on the internal margins of the foramen magnum at the base of each occipital condyle. Both foramina are posteromedially orientated. The dorsal foramen is the external opening of the condyloid canal. It is very large (3.5 mm dorsoventral width) and its ventral margin opens into a short, posteriorly directed sulcus. The second foramen (the opening for the hypoglossal nerve) is anteroventral to and smaller than the condyloid foramen.

A 4 mm wide condylar fossa extends between the occipital condyle and the paroccipital process. The posterior edge of the right paroccipital process is incomplete. The paroccipital processes are rounded and project posteroventrally to a level similar to that of the mastoid process but well short of the ventral margin of the occipital condyles (Fig. 3C). The processes are similar to those in *W.*

vanderleuerei. A small condyloid foramen occurs on the posterior surface of the paroccipital just dorsal to the condyloid fossa. The ventral surface of the paroccipital process has an angular lateral edge which abuts the mastoid process (Fig. 4A). The anterolateral margin of the paroccipital process forms a slight projection over the mastoid process. Anteriorly, the paroccipital is separated from the posterior end of the periotic by a broad sinus (approx. 25 mm wide). Medially, the exoccipital fuses with the basioccipital. Near the lateral margins of the occiput the mastoid forms a relatively broad crescentic band (approx. 10.3 mm wide) between the paroccipital and the narrow lateral squamosal margin (Fig. 3C). The dorsomedial half of the mastoid surface forms part of the lateral fossa of the occiput.

Auditory region. The auditory ossicles and ectotympanics are missing. In ventral and lateral aspect the outer ear canal is very broad (approx. 8 mm anteroposterior width). The canal walls are formed by the squamosal. The anterior wall of the canal is formed by the posterior surface of the postglenoid process. A broad (4 mm wide), shallow sulcus extends from the medial margin of the postglenoid process into the postglenoid cavity. The postglenoid cavity is large and extends anteriorly and dorsally, as is the condition in *P. roskellyae*, although in that species it expands laterally into the postglenoid process. It differs from *W. vanderleuerei* where it is instead divided by a horizontal septum. At its posteromedial margin there is a small, deep, oval fossa into which opens the canal from the subsquamosal fossa. A narrow transverse sulcus courses across the anterior wall of the postglenoid cavity and connects (piercing the fossa's anterior wall on the left side) with this fossa. At the ventral margin of this fossa is a small, posteriorly opening postglenoid foramen. The postglenoid cavity is separated from the squamosal hypotympanic sinus by a thick septum from which projects a small spur at approximately the septum's midpoint.

The posterior wall of the outer ear canal bears a large laterally orientated sulcus, the stylomastoid notch. Immediately dorsal to this notch, the wall of the canal forms a small fossa that is bounded dorsally by a small transverse crest. This fossa would have been a recess for the dorsal flank of the ectotympanic.

Periotic. The periotic (Fig. 4A) sits in a large sinus that is bordered medially by the basioccipital, laterally by the squamosal, anteriorly by the alisphenoid and posteriorly by the paroccipital process. In lateral view, the periotic is subrectangular in shape with its long axis (14 mm long) oriented in an anteroventral–posterodorsal direction. In ventral view the periotic is roughly triangular; it is narrow and flattened anteriorly and becomes rounder and broader posteriorly. Three fenestrae occur on the dorsal margin of the tympanic face: the central opening, the fenestra vestibuli, is horizontally oval and opens laterally;

posteroventral to the fenestra vestibuli is the large foramen of the fenestra cochleae which is semicircular and posteriorly orientated; anterodorsal to the fenestra vestibuli is the small foramen for the facial nerve (secondary facial foramen) which is dorsoventrally oval and opens posteriorly. A broad sulcus courses posteriorly from this foramen across the dorsal margin of the fenestra vestibuli. Ventral to the fenestra vestibuli and anterior to the fenestra cochleae, a large prominent rostral tympanic process projects from the ventrolateral portion of the periotic. The periotic of *W. vanderleueri* also has a prominent rostral tympanic process. In *P. roskellyae* this process is smaller and more obtuse. In lateral view, this process can be seen lying between the alisphenoid tympanic wing anteriorly and the mastoid process posteriorly. The process is rounded ventrally, and narrows laterally to a blunt point.

Anterolateral to the secondary facial foramen the periotic forms a narrow epitympanic wing that is bordered anterodorsally by the roof of the squamosal epitympanic sinus, and medially appears to extend beneath the edge of the squamosal. Lateral to the secondary facial foramen, the periotic forms a deep incudal fossa. Posterior to the incudal fossa and lateral to the fenestra cochlea is the fossa for the stapedius muscle. A low, rounded septum separates these two fossae. The stapedial fossa is deep and bears two anterior depressions. A large sinus, the tympanic sinus (= the mastoid epitympanic sinus of Archer 1976a) separates the posterior end of the periotic from the paroccipital. At the medial end of this sinus is a large, deep, transverse sulcus that forms the posterior lacerate foramen.

Mastoid. The mastoid part of the periotic is developed posteriorly into an elongate process (Fig. 4A). The lateral wall of the stapedial fossa forms the medial edge of the mastoid process. The posterior margin of the fossa forms a small ridge that extends posterolaterally to the mastoid process (the caudal tympanic process). In ventral view, the mastoid is narrow anteromedially and widens laterally to form a rounded, obtuse process. The posterior edge of the left mastoid process is quite rugose and bears a number of small tubercles. On the medial edge of the ventral surface, a small transverse sulcus courses into the tympanic sinus. Anteriorly, the mastoid makes a broad contact with the squamosal.

Dentition

The dentition of *Wakaleo schouteni* exhibits the characteristic thylacoleonid morphology of a bladed third premolar and bunodont, crenulated, molars. The number of premolars is variable and may be one, two (Figs 2A, 5A) or three (Fig. 5D, E). There are four molars, as in *Priscileo*, and unlike in *W. oldfieldi*, *W. vanderleueri* and *W. alcootaensis*, which exhibit loss of the posterior molars.

Upper dentition. The upper dentition of QM F45200 (Fig. 5A–D) shows considerable wear and description is assisted by referral to other specimens where appropriate (Fig. 5E, F). Dental measurements are provided in Supplemental Tables 1a and 1b.

Incisors. There are alveoli for three incisors but none are preserved. The alveoli in order of decreasing size are I^1 , I^3 , and I^2 . The I^1 is alveolus is oval and is twice the dimensions of the I^3 alveolus. The I^2 is alveolus is slightly smaller than the I^3 alveolus.

Canines. The canines (QM F23443, Fig. 5D) are short, recurved slightly, and have a broad, oval base. The primary cusp is anteriorly situated. The lingual and buccal surfaces are separated by a small longitudinal ridge that ascends anteriorly and posteriorly from the tip of the canine to its root. Enamel is present on the apical half of the crown on both the lingual and buccal surfaces. At the level of the alveolus the root of the canine curves almost horizontally into the tooth socket. The canines resemble those of *W. vanderleueri* and *W. alcootaensis* (Yates 2015) and are unlike those of *Thylacoleo carnifex* which are relatively smaller and more peg-like. The canine alveoli are proportionally larger than those of *P. roskellyae* relative to the length of the C–P³ diastema.

Premolars. The presence of P¹ and P² is variable. QM F 23443, QM F23446 and QM F57945 exhibit alveoli for P¹ and P² (Fig. 5D, E). The size and positions of these alveoli, relative to the canine and P³, are similar to those of the anterior premolars in *P. roskellyae*. In contrast, the holotype, QM F45200, lacks an alveolus for P¹ and, QM F24680 and QM F57314 lack alveoli for both P¹ and P², bearing pits in the diastema which more closely resemble foramina than true alveoli. *Wakaleo vanderleueri* (and probably *W. oldfieldi*) also exhibits loss of an anterior premolar. In *W. vanderleueri* the single anterior premolar alveolus is located near the midpoint of the diastema.

P¹. Variably present. An alveolus for P¹ is present in QM F23443 (Fig. 5F), QM F23446 (Fig. 5E) and QM F57945. P¹ is single-rooted and its alveolus is larger than that of P².

P². Variably present. It is single-rooted and situated at the base of P³. Its alveolus is smaller than that of P¹ (Fig. 5E, F).

P³. QM F45200 only preserves the left P³ which is heavily worn (Fig. 5A, B). P³ is sectorial. It has anterior and posterior cusps that are linked by a longitudinal blade that is notched so that in profile the complete cutting edge is W-shaped. In these features it resembles the P³ of *W. oldfieldi*, *W. vanderleueri* and *P. roskellyae* (Gillespie 1997; Murray *et al.* 1987; Gillespie *et al.* 2014). The anterior and posterior cusps are subequal in height. An anterior crest extends from the anterior cusp to the base of the

crown where it curves anterolingually and becomes thicker. On the lingual flank, an anterolingual crest extends from the anterior cusp and forms a prominent rounded cusplule on the basal half of the crown. This cusplule is larger in other species of *Wakaleo* and is lacking in *P. roskellyae* (Archer & Rich 1982; Gillespie 1997; Murray *et al.* 1987; Gillespie *et al.* 2014). A narrow, fluted valley lies between the anterior crest and the anterolingual crest. The lingual surface below the posterior cusp is broadly convex.

The anterior buccal surface is greatly rounded as in other species of *Wakaleo* and in contrast to *P. roskellyae*. On the buccal flank, crests from the two major cusps converge to form the margins of a broad, v-shaped valley. The posterior portion of the longitudinal blade that connects the posterior cusp to the posterior margin of the tooth is occlusally concave. A near-vertical posterobuccal crest occurs at the posterior end of the blade. It forms the posterior edge of a small buccal basin that is between the posterior cusp and posterior end of the crown.

The two roots are relatively similar in size to those in *W. oldfieldi*, are much larger than those in *P. roskellyae*, but not as massive as those in *W. vanderleueri*. *Wakaleo vanderleueri* differs in having a relatively larger anterior root such that the crown barely bulges anteriorly beyond the root and it has greater lingual inflation, resulting in the loss of lingual constriction of the crown posterior to the anterolingual cusplule.

Upper molars. In all maxillae except one (QM F23446), there are four molars that decrease in size posteriorly. The molar gradient is less steep than it is in *W. vanderleueri*. In general, the molar morphology of *W. schouteni* is most similar to *W. oldfieldi* and *W. vanderleueri*. Features shared with these species include M^1 with an enlarged metacone and a stylar basin with a low and buccally displaced margin, and M^2 with a lingually displaced paracone and metacone, reduced trigon basin width relative to crown width and a relatively posteriorly situated protocone.

M^1 . In QM F45200 both M^1 s are heavily worn and the right M^1 is only partially preserved. Hence, description of this molar has also involved referral to QM F30250, an unworn M^1 (Fig. 5G). M^1 is nearly trapezoidal and most similar to M^1 of *Wakaleo oldfieldi* and *Priscileo roskellyae*. This shape is the result of greater development of the posterolingual corner of the crown. In contrast, M^1 in *Wakaleo vanderleueri* is more triangular. The crown is dominated by a broad, relatively deep, trigon basin that bears numerous radial crenulations. The metaconule is relatively small. However, it is better developed than that cusp in *W. oldfieldi* and *W. vanderleueri*, but not as well developed as it is in *P. roskellyae*. The paracone is taller than the metacone and connected to the latter by a longitudinal blade that is notched midway along its length. The

height of these cusps and their connecting blade results in the buccal half of the crown being topographically much taller than the lingual half. The lingual flank of the longitudinal blade is steep. A short preparacrista connects the paracone to the anterior margin where it joins an anterobuccal crest that continues to the anterobuccal base of the crown. In QM F45200 a small cusp (stylar cusp B or parastyle?) occurs on this anterobuccal crest. This region of the crown abuts the posterior edge of P^3 , allowing the preparacrista to be contiguous with the longitudinal blade of P^3 . An anteriorly convex preparaconulecrista occurs on the lingual flank of the paracone. This crest thickens lingually and terminates at a notch midway to the protocone. A wear facet occurs where the crest is thickened and possibly indicates the location of a paraconule. The protocone is well developed and its rather bulbous base dominates the lingual edge of the crown. In *W. oldfieldi* and *W. vanderleueri* the protocone occurs slightly more posteriorly but in *P. roskellyae* it is relatively more anterior. A short preprotocrista extends towards the paraconule and with the preparaconulecrista forms the anterior margin of the trigon basin. The postprotocrista and premetaconulecrista form the lingual margin of the basin. In QM F30250 these crests are separated by a small notch midway between the protocone and metaconule, but in worn specimens they connect. The metacone has a broad conical base, which is the condition in other species of *Wakaleo*, but this cusp is better developed than it is in *P. roskellyae*. As in *W. oldfieldi* and *W. vanderleueri*, a short postmetacrasta extends posteriorly. In *P. roskellyae* the postmetacrasta is deflected posterobuccally. A crescentic lingual metacrasta occurs on the lingual face of the metacone, terminating approximately two-thirds of the way to the metaconule. In *P. roskellyae* this crest is straight and much shorter. In QM F30250, a short crest that is formed by a series of small ridges extends from the metaconule towards the lingual metacrasta. This crest is also present in *W. oldfieldi*. In worn specimens these appear as a single transverse crest connecting the metacone and metaconule. As in *W. oldfieldi* and *W. vanderleueri* the metaconule is weakly developed, unlike *P. roskellyae*, which has a better developed cusp. A small posterior cingulum links the postmetacrasta to the postmetaconulecrista. The stylar shelf is relatively broad and bears a basin that extends to the buccal edge of the crown. The stylar basin is broader anteriorly and posteriorly narrowed because of the expanded metacone. The edge of the basin is well below the apices of the paracone and metacone. This is also the condition in *W. oldfieldi* and *W. vanderleueri* and is unlike *P. roskellyae* in which the edge of the basin is closer to the postparacrista and is much taller relative to the paracone and metacone. Numerous transverse ridgelets line each side of the buccal edge of the stylar basin. On the buccal flank of the crown, the valley that occurs above the junction of the roots is variably developed; a small vertical ridge is

present in QM F30250; however, QM F45200 bears a broad swelling in this region. As in other species of *Wakaleo* and unlike *P. roskellyae*, the lingual root is greatly exposed.

M². In QM F45200 and QM F23443 (Fig. 5F), this molar is heavily worn and description is assisted by QM F23801 (Fig. 5H). M² is generally similar to M¹ but exhibits the following differences. It is slightly smaller, proportionately shorter, and more heart-shaped. The antero-buccal corner is more rounded and lacks the angularity of M¹. Although the paracone and metacone are relatively tall, the height difference between the buccal and lingual margins is less extreme. The paracone is relatively more lingual in relation to the buccal edge and is less anterior relative to the protocone. In most worn specimens the lingual half of the anterior cingulum is obscured by the extensive wear facet on the protocone; however, the unworn QM F23801 indicates it extends toward the protocone, as in M¹. The preparaconulecrista bears crenulations on its anterior and posterior flanks and a distinct paraconule cannot be discerned. In QM F23801 and QM F45200 the postparacrista and premetacrista are separated by a narrow fissure at the notch of the longitudinal blade that their conjunction forms. The metacone is smaller and is much closer to the posterior margin; hence, the postmetacrista is much shorter. In QM F23801 the lingual metacrista intersects crenulations of the trigon basin about two-thirds of the way to the metaconule and in worn specimens it appears to be linked to this cusp. The crown is relatively narrower between the lingual metacrista and the posterior margin. In QM F23801, the postmetaconulecrista is short and curves toward but fails to meet the lingual metacrista. In worn specimens it merges with edge of the posterior cingulum. The metaconule is very weakly developed and appears as a small bump near the postero-lingual corner of the trigon basin (QM F23801 and QM F24680). The crown below the paracone is more buccally expanded which results in the anterior half of the stylar shelf being relatively broader than in the M¹. A vertical valley in the middle of the buccal flank of the crown pinches the stylar shelf so that its buccal edge, in most cases, deflects toward and meets the longitudinal blade at its notch. This results in the shelf consisting of two small basins rather than a single long basin. Large transverse crenulations may also be associated with the constriction of the stylar shelf (QM F24680). The trigon basin has prominent radial crenulations.

M³. Description is assisted by QM F23443 (Fig. 5F), QM F23444 and QM F40206. M³ is triangular, has a simple basin-like crown and is similar to other species of *Wakaleo* (Murray *et al.* 1987; Gillespie *et al.* 2014). It differs from M¹ and M² in lacking a stylar shelf. The paracone is the tallest cusp and the protocone and metacone are subequal in height. These cusps are connected by a

crest that completely encircles the crown and forms the margins of the trigon basin. The extensively crenulated trigon basin causes this crest to be corrugated in some areas. A small crest (obscured by wear in most specimens) extends lingually from the paracone toward the protocone and deflects anteriorly to join the anterior margin just before the protocone. A short cingulum occurs anterior to this crest. There are three roots; the medial root is the largest, and the posterior is slightly larger than the anterior.

M⁴. This is similar to M³ but lacks an anterior cingulum (Fig. 5A, B). It is triangular and the surface of the trigon basin is highly crenulated (QM F23458). The protocone is taller than the metacone and paracone which are subequal in height. M⁴ has three roots; the medial is slightly larger than the subequal anterior and posterior roots.

Dentary. The morphology of the dentary and lower dentition of *W. schouteni* is most similar to that of *W. oldfieldi* and *W. vanderleueri* (Clemens & Plane 1974; Megirian 1986; Murray & Megirian 1990) but differs from these species in being smaller and possessing an extra tooth between I₁ and P₃ and an M₄. Right dentary QM F52247 is the most complete and preserves the horizontal ramus, coronoid process, masseteric fossa and angular process (Fig. 6A–C).

QM F52247 measures 98.2 mm in length from the edge of the I₁ alveolus to the posterior rim of the articular condyle. In lateral view, the horizontal ramus tapers anteriorly between P₃ and I₁ and is deepest below the posterior root of P₃ (Fig. 6A, B). In dorsal view (Fig. 6D), the tooth row forms a gentle arc as in *W. oldfieldi* and *W. vanderleueri*.

The anterior end of the horizontal ramus is dominated by the alveolus for I₁, the space for which fills the anterior region of the dentary. This alveolus is deep and laterally compressed. Between the I₁ alveolus and P₃, the dorsal surface bears two small alveoli (Fig. 6D, E). The anteriormost alveolus is elongate and is approximately 5 mm posterior to the I₁ alveolus. It opens into an anteriorly directed sulcus which suggests that the tooth was elongate. The second alveolus is small and oval and is just anterior to or at the base of P₃. It opens anterodorsally and is relatively shallow. It probably held a small, single-rooted P₂. In this region in *Wakaleo oldfieldi* and *W. vanderleueri* there is one alveolus and in *P. roskellyae* there are three. The anteriormost alveolus in *W. schouteni* is similar in shape to the anteriormost alveolus in *P. roskellyae*. The second alveolus is similar in shape and location to the single alveolus (P₂) in *W. oldfieldi* and *W. vanderleueri*.

The symphyseal area is large, roughly rectangular, and extends posteriorly to the level of the posterior root of P₃ (Fig. 6A), but is not as tall as in *W. oldfieldi* and *W. vanderleueri*. On the lingual surface of the ramus a shallow

sulcus courses along its centre from below M_2 to the pterygoid fossa, just anterior to the mandibular foramen (Fig. 6A). As in *W. oldfieldi* and *W. vanderleuerei*, a large posteriorly directed mandibular foramen occurs at the anterior edge of the deep recess of the pterygoid fossa. The pterygoid fossa is very deep, pushing the posteroinferior part of the ramus buccally and resembles the condition in *W. oldfieldi* and *W. vanderleuerei*. The angular process extends lingually to form a horizontal, triangular shelf that extends posteriorly to, but not beyond, the posterior margin of the condyle (Fig. 6A, C). The lingual border of the shelf is steep and thick and forms a slight tuberosity at its posterior third. This is unlike the condition in *W. vanderleuerei* in which the lingual edge of the angular process protrudes lingually and bears a triangular, dorsally projecting process.

The buccal surface of the horizontal ramus is gently convex. As in *W. oldfieldi* and *W. vanderleuerei*, a large anterodorsally directed mental foramen occurs ventral to the anterior root of P_3 (Fig. 6B). A second, smaller, mental foramen occurs ventral to M_1 and opens posteriorly.

The coronoid process resembles that in *W. oldfieldi* and *W. vanderleuerei*; it is tall, anteroposteriorly deep, dorsally rounded and posteriorly inclined (Fig. 6A, B). In QM F52247 the apical region is fractured and laterally displaced. The depth of the ascending ramus from the top of this process to the ventral margin is 53.3 mm. The anterior edge of the coronoid process is thickened and becomes thinner dorsally. Its posterior edge is thin and ventrally extends posteriorly to form the mandibular notch directly anterior to the condylar process. The articular surface of the condyle is broad (18.1 mm), gently rounded, and lies at a level slightly dorsal to the molar row (Fig. 6A, C). In dorsal view it has a sinusoidal outline. The lingual half is thick and tapers to a point and the buccal half is thinner and rounded at its lateral extremity.

The masseteric fossa is large and extends dorsally to approximately the level of the condyle and anteriorly to the level of M_4 (Fig. 6B). A small, dorsally directed masseteric foramen occurs at the inferior third of the masseteric fossa. In *W. oldfieldi* and *W. vanderleuerei* the masseteric fossa extends much further dorsally. The dorsal limit of the fossa is marked by a small crest that curves towards the mandibular notch. Dorsal to this crest is a shallow tear-shaped fossa for the superior temporalis muscle. Ventrally, the masseteric fossa is marked by the masseteric line which extends posteriad towards the condyloid crest that descends from the condylar process. As in *W. oldfieldi* and *W. vanderleuerei*, the posterobuccal corner of the dentary extends buccally and forms a small shelf at the posterolateral margin of the masseteric fossa.

Lower dentition. *Wakaleo schouteni* is similar to *P. roskellyae* in having four molars but differs in having a dentition that is larger and has molars that are relatively

narrower and that have much deeper talonid basins and as such are more similar to that of *W. oldfieldi* and *W. vanderleuerei* (Clemens & Plane 1974; Gillespie *et al.* 2014). The paired dentaries QM F52247 preserve P_3 and M_{1-3} , and alveoli for I_{1-2} , P_2 and M_4 (Fig. 6C–E).

I_1 . Only QM F31376 and QM F30465 retain I_1 (Fig. 6F). I_1 is similar to that of *W. oldfieldi* and *W. vanderleuerei* in being procumbent and scimitar-like, laterally compressed, and having a root that extends deeply to below P_3 . It differs from *W. oldfieldi* and *W. vanderleuerei* in being slightly more gracile and in that its medial surface bears a longitudinal groove. The flatter medial surface in those species may be the result of wear between the incisors. The dorsobuccal edge of the *W. schouteni* incisor is slightly less prominent than that of *W. oldfieldi*.

The short region between I_1 and P_3 bears alveoli for two single-rooted teeth. These teeth have not been preserved. The alveolus directly posterior to I_1 is oval, horizontally directed, and is similar to the alveolus that is directly posterior to I_1 in *Priscileo roskellyae*. Its shape suggests that it represents the alveolus for either a posterior incisor or canine. The second alveolus is small, round, ventrally directed, and is close to the anterior root of P_3 . This alveolus most likely housed a single-rooted P_2 . This alveolus is similar to the single alveolus found between I_1 and P_3 in dentaries of *W. oldfieldi* and *W. vanderleuerei*.

P_3 . This is sectorial and resembles that of *W. oldfieldi* and *W. vanderleuerei* (Clemens & Plane 1974; Gillespie *et al.* 2014). It consists of a tall anterior cusp and a shorter posterior cusp that is joined by a buccally bowed longitudinal blade (Fig. 6A, B, D, E). The P_3 of *W. schouteni* is approximately three-quarters the length of *W. oldfieldi* and two-thirds that of *W. vanderleuerei*, and in comparison to these species is proportionally shorter relative to the total cheektooth row. Minor differences include having a slightly more sharply defined anterolingual crest and in having a relatively concave surface between this crest and the anterior crest, rather than a broadly convex one. It differs from *P. roskellyae* in being larger (longer by 40–50%), in having a steeper slope on the longitudinal blade and in having the posterior end of the blade meet the anterior crest on M_1 , rather than meet the anterolingual edge of M_1 . It also differs from *P. roskellyae* in having much greater exposure of the roots, in particular the anterior root. As in *W. oldfieldi*, *W. vanderleuerei* and *P. roskellyae*, P_3 abuts and is slightly overhung by the M_1 .

Molars. The molars are very similar to other species of *Wakaleo* (Clemens & Plane 1974; Megirian 1986; Murray & Megirian 1990; Gillespie *et al.* 2014).

M_1 . As in other species of *Wakaleo* and *Priscileo roskellyae*, M_1 has a trigonid that is twice the height of the talonid. M_1 in occlusal view is basically rectangular and is anteriorly slightly narrowed. The anterior edge of the

crown forms a slight lip where it abuts P_3 . The trigonid has an apical cusp that is slightly shorter than the anterior cusp of P_3 (Fig. 6A, B). As in *W. oldfieldi* and *W. vanderleueri*, three prominent blades connect to the apical cusp: an anterior blade connects the apical cusp with the longitudinal blade of P_3 ; a long buccal blade descends to the base of the crown; and a lingual blade steeply descends to meet the lingual crest of the talonid basin. The anterobuccal flank of the trigonid also bears a short anterior blade that in many specimens is flattened from wear. This blade is readily observed on unworn teeth (e.g. QM F30073 and QM F23449). The anterolingual flank of the trigonid bears two short, vertical, rounded crests. The anteriormost of these is shorter than the posterior crest which is much larger and extends to the lingual blade just lingual to the apical cusp. The posteriormost crest is relatively larger in *W. vanderleueri*. The posterior face of the trigonid is steep, triangular, and anteriorly inclined. The posterior end of the crown is relatively broader and slightly squarer than in *W. oldfieldi* and *W. vanderleueri*. The talonid basin is oval (Fig. 6D) as in those species; however, it is relatively broader and the entoconid and hypoconid are more broadly separated. It differs from *P. roskellyae* in having a talonid basin that is relatively narrower, has a convex lingual margin rather than a straight or lingually deflected margin, and also lacks the small posterolingual basin that may be present in that species.

M₂. The M_2 is similar to those of other species of *Wakaleo*; there is a tall trigonid that has a small, centrally positioned anterior basin and a larger talonid basin (Fig. 6D, F). It differs slightly from *W. oldfieldi* in being more rectangular and in having a proportionally broader talonid. It also differs from *W. oldfieldi* and *W. vanderleueri* in having a relatively broader anterior basin and markedly broader talonid basin. It differs distinctly from *Priscileo roskellyae* in having a much taller trigonid and a much narrower and medially situated anterior basin.

M₃. The M_3 is subrectangular (Fig. 6D, E). The sides of the crown are gently rounded and the occlusal surface bears a shallow, lightly crenulated talonid basin. The anterior end of the tooth is slightly taller than the posterior end. There are two roots of approximately equal size. It is most similar to M_3 of *W. oldfieldi* (Gillespie *et al.* 2014) but is relatively larger and squarer than in that species. It differs markedly from *W. vanderleueri* which has a small, oval, molar that lacks a trigonid and a talonid basin (Gillespie *et al.* 2014).

M₄. Not preserved. The alveolus is small and slightly oval. There is no evidence of a septum indicating the presence of two roots. This suggests either that the two roots were so compacted that there was no room for a septum to develop, or possibly the tooth had a single root. In either case, the tooth was only weakly anchored.

Humerus. Three humeri of *Wakaleo schouteni* have been recovered from the Riversleigh localities: QM F23443 and QM F57905, left and right distal ends, respectively, and QM F57904, a complete left humerus (Fig. 7A–F). Assignment of the humerus QM F23443 (Fig. 7A, B) to *W. schouteni* is based on the following reasons: (1) comparison to similar elements of other thylacoleonids (in particular, to that of *P. pitikantensis*) and other marsupial groups indicate its thylacoleonid affinities; (2) it was found in association with a palate of *W. schouteni* (Fig. 5F) and an edentulous dentary and other postcranial elements, all regarded as being from the same individual, in a small limestone sample; (3) the humerus is of a medium-sized mammal and is an appropriate size in relation to the size of the palate found at the site; and (4) no elements of other mammalian taxa were recovered from the sample. Assignment of the isolated bones, QM F57905 (Fig. 7C, D) and QM F57904 (Fig. 7E, F) to *W. schouteni* are based on comparisons with QM F23343. Description of the humerus of *W. schouteni* is based on the complete element QM F57904.

QM F57904 (Fig. 7E, F) is 119.7 mm in length and has a maximal distal width of 42.5 mm. It has a moderately large humeral head, a deltoid crest that extends over the proximal half of the element, and distally is broad and has a well-developed lateral epicondylar crest. The humeral head of QM F57904 is broadly rounded, slightly shorter than the greater tubercle, and taller than the lesser tubercle. The lesser tubercle of QM F57904 is appressed against the humerus head. The proximal end of the shaft has a greater anteroposterior thickness than the distal shaft. The deltoid crest extends over the proximal half of the diaphysis. The anterior surface of the crest is gently rounded and is slightly concave when viewed in profile, the distal end of the crest protruding slightly anteriorly. On the lateral edge of the deltoid crest, near its midpoint, is a small tuberosity marking the attachment site for the deltoideus pars spinalis muscle. The intertubercular groove is broad and shallow. This groove becomes deeper proximally. A narrow, 5 mm long, muscle scar marking the attachment site for the latissimus dorsi muscle occurs on the posteromedial edge of the shaft adjacent to the end of the deltoid crest. The area of the shaft proximal to the latissimus dorsi scar is smooth.

The shaft distal to the deltoid crest narrows and then broadens markedly (42.5 mm wide). The shaft spreads laterally to form a tall, straight, lateral epicondylar crest. A well-developed medial epicondyle occurs at the distomedial extremity. A large entepicondylar foramen is enclosed just proximal to the medial epicondyle. The trochlea is centrally situated, relatively broad, and gently rounded. The capitulum is strongly rounded and is slightly medial to the lateral epicondylar crest, and the olecranon fossa is very shallow.

The humeri of *W. schouteni* differ from that of *P. pitikantensis* (SAM P37720) in being generally larger distally and QM F57904 exhibits differences in proximal morphology (see below).

Wakaleo pitikantensis (Rauscher, 1987) comb. nov.

1987 *Priscileo pitikantensis* Rauscher: 424, figs 1–5.

Holotype. SAM P37719, a left maxillary fragment with partial alveoli for C–P³, broken M^{1–2}, alveoli for M^{3–4}, and two right maxillary fragments with partial alveoli for C–P³, roots of M^{1–2}, alveoli for M^{3–4}.

Revised species diagnosis. *Wakaleo pitikantensis* differs from all other species of *Wakaleo* in being smaller and, with the exception of *W. schouteni* sp. nov., in having three premolars and four molars. It differs from *W. schouteni* sp. nov. in having a humerus with the following distinguishing features: (1) humeral head that is slightly more laterally compressed, more proximally rounded, and taller than the greater tubercle; (2) lesser tubercle that is medially broad (rather than appressed against the head) and which contributes to a relatively broader proximal humeral width; (3) deltoid crest with deep anterior concavity; (4) greater development of the teres major and deltoideus pars spinalis tubercles; and (5) a more distal, lower-angled enclosure of the entepicondylar foramen.

Wakaleo schouteni differs from *W. pitikantensis* comb. nov. in having a relatively longer diastema between the canine and P¹. The humerus differs from that of *W. pitikantensis* in having: the humeral head broader and less proximally rounded; lesser tubercle appressed against the humeral head; greater tubercle that is taller than the humeral head; deltoid crest that lacks anterior concavity; shaft that lacks development of the teres major and deltoideus pars spinalis tubercles; and steeper enclosure of the entepicondylar foramen.

Referred specimens. SAM P37720, fragments of right nasal and jugal, proximal right scapula lacking spine, left humerus, right radius, distal left radius, four rib fragments, left magnum, left ectocuneiform, phalanx. UCMP 88457, a crushed right humerus.

Occurrence. The holotype is from UCMP locality V-5857, south-western end of Lake Pitikanta (faunal zone C of the Etadunna Formation), Tirari Desert, South Australia (Rauscher 1987), which is estimated to be late Oligocene in age (Woodburne *et al.* 1993).

Remarks. The similarities of the dental formula, M² morphology, and size of *Priscileo pitikantensis* Rauscher, 1987 with *W. schouteni* warranted a reassessment of the holotype (SAM P37719) and its associated humerus (SAM P37720).

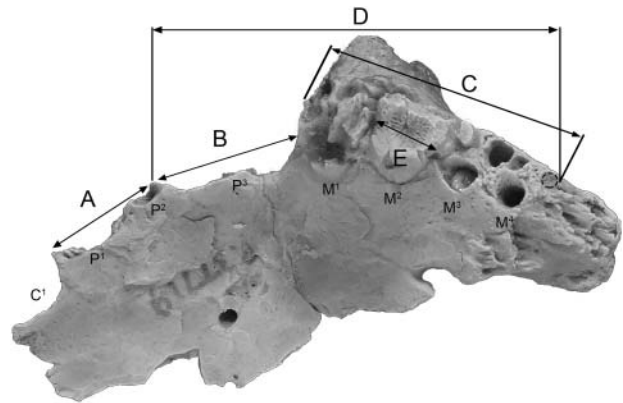


Figure 8. Measurements of alveoli and M² mid-crown length for comparison of SAM P37719 (pictured), *Priscileo roskellyae* and species of *Wakaleo* shown in Table 2.

The limited amount of material for the holotype of *Priscileo pitikantensis* (SAM P37719) restricts comparative dental measurements (Fig. 8, Table 2). The positions of the single-rooted anterior premolars (P¹ and P²) in SAM P37719 are similar to those of *Wakaleo schouteni* sp. nov. (QM F23443, QM F23446 and QM F57945), i.e. P¹ occurs midway between C¹ and P² and P² is situated at the base of P³. In *Priscileo roskellyae*, P¹ is relatively closer to P² than to C¹. In SAM P37719 the lingual margin of the P³ alveolus forms an acute angle to the lingual margin of the molar row which is similar to that in *W. schouteni* sp. nov. and *W. vanderleuerei* and is more acute than the angle in *P. roskellyae*.

Comparative measurements show that SAM P37719 is smaller than other species of *Wakaleo* and approaches the size of *W. schouteni* sp. nov. (Table 2). SAM P37719 is distinctly larger than *P. roskellyae* in all dental measures (Table 2). Compared to the average values for *W. schouteni* sp. nov., SAM P37719 is 10% shorter in P³–M⁴ length and approximately 17% shorter in C¹–P³ length and P³ alveolus length. Similarly, the humerus of *P. pitikantensis* (SAM P37720) is generally smaller than that of *W. schouteni* (Table 3). It is distally narrower than all *W. schouteni* specimens except QM F57904 which it only just exceeds in width but is 8% shorter in total length.

Only the protocone, paracone, and crenulated trigon basin of M² are preserved in SAM P37719. The remains of this crown show greater similarities to the M² of *Wakaleo schouteni* sp. nov., *W. oldfieldi* and *W. vanderleuerei* than to the M² of *Priscileo roskellyae*. These similarities include the following:

1. The trigon basin is relatively triangular primarily because of the posterobuccally directed postprotocrista. In *P. roskellyae* the postprotocrista is more posteriorly directed and the trigon basin extends posterolingually, resulting in a squarer basin.

Table 2. Comparative measurements (in mm) of alveoli and M² length for SAM P37719, *Priscileo roskellyae* and species of *Wakaleo*.

Species Specimen No.	A C ¹ –P ³ diastema	B P ³ alveolus length	C M ¹ a–M ⁴ a length	D P ³ a–M ⁴ a length	E M ² length midcrown
<i>Priscileo roskellyae</i>					
QM F23453*	6.9	9.1	15.5	23.5	4.2
<i>Wakaleo pitikantensis</i> comb. nov.					
SAM P37719	9.6	11.2	[22.0]	31.3	5.5
<i>Wakaleo schouteni</i> sp. nov.					
QM F45200*	11.9	12.3	23.3	34.2	5.8
QM F23443*	12.4	13.9	23.3	35.8	5.5
QM F24680	[10.9]	13.2	24.0	35.7	6.2
QM F57314	—	15.1	[25]	35.6	—
QM F23446	12.9	12.6	20.2	32.0 [^]	5.8
QM F57945	9.9	13.3	21.8	33.3	5.8
QM F57311	—	—	[24]	—	[5.6]
QM F30378	—	—	—	—	6.2
QM F52252	—	—	—	—	5.9
QM F20573	—	—	—	—	5.7
QM F23801	—	—	—	—	6.6
<i>n</i>	5	6	7	6	10
Mean	11.6	13.4	23.0	34.4	5.9
Range	9.9–12.9	12.3–15.1	20.2–25	32.0–35.8	5.5–6.6
<i>Wakaleo oldfieldi</i>					
QM F24745	—	—	—	—	7.5
QM F31398	—	—	—	—	7.1
<i>Wakaleo vanderleueri</i>					
CPC 26604*	11.7	20.1	24.2	41.1 [^]	6.6

Abbreviations: a = alveolus; [] = estimate; * = average of left and right; [^] = measurement to M³ because M⁴ is lost.

- The crown below the protocone is relatively bulbous and deep. In *P. roskellyae* the crown supporting the protocone is less bulbous and the protocone has a relatively more anterior position.
- The crown below the metaconule does not extend lingually and results in an outline that is roughly triangular. In *P. roskellyae* the posterolingual corner of

- the crown is better developed, the metaconule is relatively more lingual and the crown is less triangular.
- The trigon basin is relatively narrow with respect to crown width. In SAM P37719 the buccal flank of the trigon basin is relatively steep and it is likely that the longitudinal crest that would have marked its buccal margin lies very close to its fractured edge. The distance between the broken edge of the trigon basin and the buccal edge of the roots indicates the buccal flank (stylar shelf) was relatively broad. The trigon basins of M² in species of *Wakaleo* also have a steep buccal flank and the crowns have a moderately broad stylar shelf. In *P. roskellyae* the stylar shelf of M² is relatively narrow and the trigon basin extends to within a short distance of the buccal margin of the crown.
- The paracone is situated medially relative to the buccal edge of the anterobuccal root.
- The posterior margin of the trigon basin is relatively straight. In *P. roskellyae* the lingual meta-crista forms an anteriorly bowed crest.

Table 3. Measurements (in mm) of humeri of SAM P37720 and *Wakaleo schouteni* sp. nov.

Species Specimen no.	Length	Proximal width	Distal width	Lat. epicondylar crest height
<i>Wakaleo pitikantensis</i> comb. nov.				
SAM P37720	109.8	32.1	43.1	36.5
<i>Wakaleo schouteni</i> sp. nov.				
QM F57904	119.7	29.8	42.5	35.5
QM F57905	—	—	49.1	39.4
QM F23443	—	—	52.9	46.0
<i>n</i> = 3 Mean			48.1	40.3

7. There is a large exposure of the lingual root below the protocone.
8. The canine alveolus is relatively large in relation to the C^1 – P^3 interval, as it is in species of *Wakaleo*. Furthermore, the heavy wear facet on the anterior edge of the protocone is identical to the area of wear on M^2 s of other species of *Wakaleo*. In *P. ros-kellyae* and *Microleo attenboroughi* the area of heaviest wear on M^2 is in the centre of the trigon basin.

Comparison of the *Priscileo pitikantensis* humerus (SAM P37720) with those of *Wakaleo schouteni* sp. nov. (Fig. 9) and *Thylacoleo carnifex*, the only other thylacoleonids for which humeri are known, reveals overall greatest similarity with *W. schouteni*. Although there are some differences in the development of the tubercles in relation to the humeral head and in development of some of the muscle attachments, the near identical morphology of the

distal articular facets (trochlea and capitulum) and the olecranon fossae suggest a relationship that is at least congeneric. In contrast, notwithstanding the size difference, the humerus of *Thylacoleo* has disproportionately taller distal facets and a more medially situated trochlea.

In contrast to the humerus of *W. schouteni* (QM F57904), the humeral head of SAM P37720 is more prominently rounded and is taller than the tubercles (Fig. 9C–F). SAM P37720 also differs in having a much broader lesser tubercle whereas in QM F57904 it is appressed against the humerus head (Fig. 9E–H). The differences in the development of the lesser tubercle results in the proximal end of the shaft of SAM P37720 being distinctly broader than that of *W. schouteni*. SAM P37720 further differs from QM F57904 in having a deeply concave anterior surface on the deltoid crest and a much larger and more distinctive attachment point for the deltoideus pars spinalis muscle (Fig. 9C, D, I, J). In SAM P37720 the scar marking the attachment site for the latissimus dorsi is more extensive and spreads

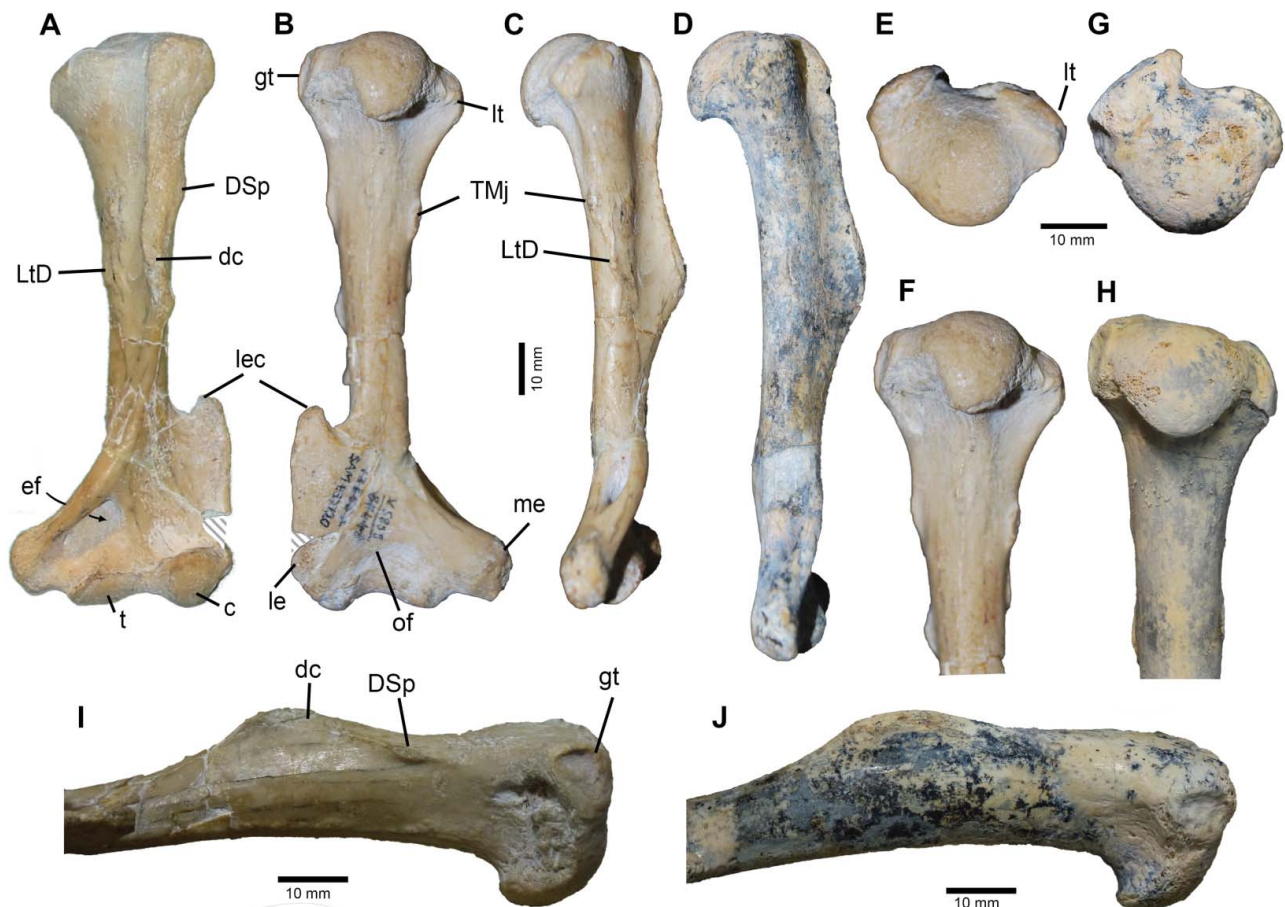


Figure 9. Comparison of the humeri, SAM P37720 from Lake Pitikanta, South Australia and QM F57904 from Riversleigh, Queensland. A–C, E, F, I, SAM P37720; A, anterior view; B, posterior view; C, medial view; E, dorsal view; F, posterior view of proximal end; I, lateral view of proximal end. D, G, H, J, QM F57904; D, medial view; G, dorsal view; H, posterior view of proximal end; J, lateral view of proximal end. Abbreviations: c, capitulum; dc, deltoid crest; DSp, deltoid pars spinalis tubercle; ef, entepicondylar foramen; gt, greater tubercle; LtD, latissimus dorsi rugosity; le, lateral epicondyle; lec, lateral epicondylar crest; lt, lesser tubercle; me, medial epicondyle; of, olecranon fossa; t, trochanter; TMj, teres major tubercle. Scale bar = 10 mm.

onto the anterior surface (Fig. 9A, C). The area of the shaft proximal to the latissimus dorsi scar on SAM P37720 bears a broad area of scarring and a small but prominent, medially projecting tuberosity marking the attachment site of the teres major muscle and is unlike QM F57904 which has a smooth, scar-free surface (Fig. 9A, C, D).

On the basis of the overall similarities of its M^2 with that of *Wakaleo schouteni* sp. nov., *W. oldfieldi* and *W. vanderleueri*, and of its humerus with that of *W. schouteni* sp. nov., *pitikantensis* Rauscher, 1987 is referred here to the genus *Wakaleo*. The generic name *Priscileo* is therefore regarded as a junior synonym of *Wakaleo* Clemens & Plane, 1974. In contrast, ongoing research indicates that ‘*Priscileo*’ *roskellyae*, originally described on the basis of its upper dentition, demonstrates generic level differences in its cranial and dental morphology from species of *Wakaleo* and *Thylacoleo*. Taxonomic reassessment of this species is in progress.

Results

Phylogeny

Our analysis recovered three most-parsimonious trees of 132 steps (consistency index = 0.780; retention index = 0.817; rescaled consistency index = 0.638). The strict consensus tree (Fig. 10) recovers *Wakaleo* as monophyletic but with weak bootstrap support (51%). The relationships of *Wakaleo pitikantensis* and *W. schouteni* to each other and to the remaining species of *Wakaleo* are unresolved. It is likely that the high levels of missing data for *W. pitikantensis* contributed to the weak support value for

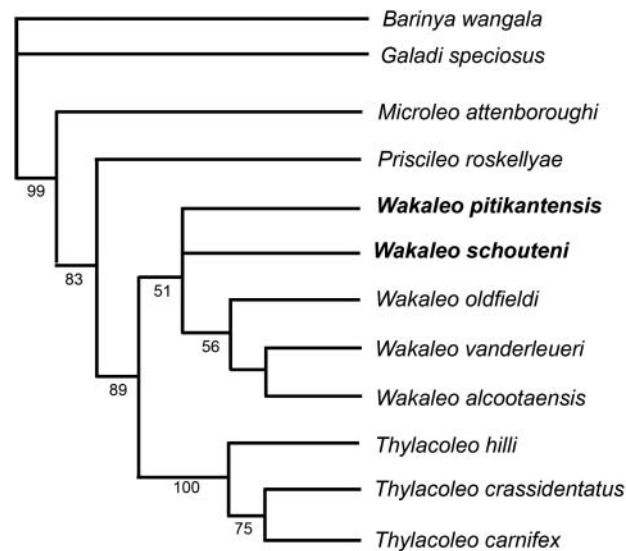


Figure 10. Strict consensus tree of three most parsimonious trees (TL = 132; CI = 0.780; RI = 0.817; RCI = 0.638; see supplemental material for character matrix). Bootstrap support values are indicated next to the internodes.

the *Wakaleo* clade. Our results differ from those of Gillespie *et al.* (2016) which placed *Wakaleo pitikantensis* (recognized as *Priscileo pitikantensis* in that analysis) outside the *Wakaleo* clade. These differences can be attributed to the addition of *W. schouteni* and new, as well as revised, characters to the data matrix.

The placement of the *Wakaleo* clade as a sister taxon to *Thylacoleo* (89% bootstrap support) is in agreement with previous phylogenies (Archer & Dawson 1982; Archer & Rich 1982; Rauscher 1987; Gillespie *et al.* 2016).

Body mass

The total skull length variable (TSL = 164 mm) employed in the regression equations of Myers (2001) resulted in body mass estimates of 22.6 kg and 24.0 kg for *Wakaleo schouteni*.

Discussion

The new thylacoleonid material recovered from FZ A and FZ B assemblages of the Riversleigh WHA is referred to *Wakaleo* on the basis of dental and cranial morphology, involving many synapomorphic features shared with other species of *Wakaleo* and in particular with *W. vanderleueri*. These features include: large sagittal and nuchal crests, well-developed supraorbital processes, lateral pterygoid processes of the alisphenoid, shallow and concave pterygoid fossa, a medially confined postglenoid cavity that does not invade the postglenoid process, a large rostral tympanic process on the periotic, cheekteeth with exposed roots, anterolingual cuspule on P^3 , large metacone on M^{1-2} , and narrowed and deep talonid basins on the lower molars.

At the time of its description, the holotype of ‘*Priscileo*’ *pitikantensis* Rauscher, 1987 differed significantly from other known thylacoleonids, being markedly smaller and having a relatively more plesiomorphic dental formula (three premolars and four molars). Since its description, three more thylacoleonid species that also possess this primitive condition have been described (*Microleo attenboroughi*, ‘*Priscileo*’ *roskellyae* and *Wakaleo schouteni*). Consequently, the condition is no longer diagnostic at the generic level. The limited material of *P. pitikantensis* restricts assessment of possible generic diagnostic characters. However, enough of its M^2 is preserved to indicate that it exhibits derived features found in the M^2 of *Wakaleo* species, i.e. reduced trigon basin width relative to crown width, broad styler shelf, deep bulbous crown below the protocone, and tall, exposed roots. Referral to *Wakaleo* is also supported by the strong morphological similarities of its humerus with that of the new Riversleigh taxon. Although *Priscileo pitikantensis* is synonymized with *Wakaleo*, ‘*Priscileo*’ *roskellyae*

demonstrates differences in cranial and dental morphology that support its generic distinction and generic revision of this taxon; these differences include a relatively shallow skull, small sagittal and nuchal crests, lack of a well-developed rostral tympanic process on the periotic, stylomastoid sulcus within the mastoid of the periotic, an extra tooth between the I_1 and P_3 , and molars with much broader trigon and talonid basins (Gillespie *et al.* in prep.).

With attribution of SAM P37719 to *Wakaleo*, consideration was given to its possible conspecificity with Riversleigh's *W. schouteni*, given their similar size. The differences in the morphology of the proximal humerus of *W. pitikantensis* and *W. schouteni* are greater than the intraspecific variation observed in samples of the humeri of the Pleistocene thylacoleonid *Thylacoleo carnifex*, the koala (*Phascolarctos cinereus*), spotted cuscus (*Spilocuscus maculatus*), brushtail possum (*Trichosurus vulpecula*) and the mountain brushtail possum (*Tr. caninus*), and greater than interspecific differences observed in the humeri of the latter two species. The differences in the humeri of the two *Wakaleo* species possibly reflect differences in the functional demands on their forelimbs.

The size differences within the *Wakaleo schouteni* humeri sample (24% for distal width, 29% for lateral epicondylar crest height) are larger than those observed in a sample of humeri of *Thylacoleo carnifex* from Naracoorte Caves, South Australia (21% for distal width; see Supplemental Table 2). Although metric studies of the dentition of *T. carnifex* fail to show a bimodal distribution (Archer & Dawson 1982; Finch & Freedman 1982), Archer & Dawson (1982) note that sexual dimorphism is a likely explanation for the significant differences observed in the size of skulls and mandibles of that species collected from Wellington Caves, New South Wales (Archer & Dawson 1982, fig. 1). The small sample of humeri of *T. carnifex* examined in this study was insufficient to allow a meaningful statistical analysis for bimodality. However, the relatively large size difference in the humeri of *W. schouteni* suggest it too may have been sexually dimorphic. Sexual dimorphism is a common phenomenon in many marsupials (Van Dyck & Strahan 2008). For example, males of the larger species of extant kangaroos have been found to be twice the weight of the largest females and may have forearms that are 10–40% longer than those of females (Jarman 1989).

Although loss of the anterior upper premolars cannot be used to separate the genera *Wakaleo* and *Priscileo*, it can be used to assess relationships within *Wakaleo* and suggests that *W. pitikantensis* and *W. schouteni* are plesiomorphic with respect to the other species in the genus. In contrast to *P. roskellyae*, species of *Wakaleo* exhibit loss of an anterior lower premolar and hence this character is a possible synapomorphy for the genus. However, it has been considered to be an ambiguous character by the analysis probably because of the lack of data for *W. pitikantensis*. Our phylogenetic analysis supports most previous

phylogenies, placing *Priscileo* as the sister taxon to a *Wakaleo*+*Thylacoleo* clade (Rauscher 1987; Gillespie 2007; Yates 2015; Gillespie *et al.* 2016). The position of *Wakaleo alcootaensis* within *Wakaleo* differs from that of Yates (2015) which placed this species as the plesiomorphic sister taxon to a *W. oldfieldi* + *W. vanderleuerei* clade. This difference results from the different outgroup taxa used in the analyses and the resulting differences in interpretation of the character states in relation to the lower anterior premolars. Our analysis used dasyurid and peramelemorphian taxa (*Barinya* and *Galadi*, respectively) as outgroups because they have dentitions generally regarded as exhibiting features that are plesiomorphic within the marsupial radiation, such as multiple lower incisors and multiple premolars (Archer 1976b, 1984). Hence, we regard premolar reduction as a derived condition. In contrast, in the analysis of Yates (2015), two of the outgroup taxa (the phascolarctid *Nimiokoala greystanesi* and the wynyardiid *Namilamideta albivenator*) lack teeth between I_1 and P_3 . This condition was therefore regarded to be plesiomorphic. Hence, *Wakaleo alcootaensis*, which also lacks teeth in this region, was interpreted as exhibiting the primitive state, whereas the presence of a single alveolus in *W. oldfieldi* and *W. vanderleuerei* was interpreted as a derived condition. The presence of two teeth in this region in the geologically older thylacoleonids *W. schouteni* and *P. roskellyae* lends support to the interpretation of premolar reduction as an apomorphic condition for thylacoleonids.

Wakaleo schouteni and *P. roskellyae*, from late Oligocene assemblages at Riversleigh, and *W. pitikantensis* from late Oligocene sediments of the Etadunna Fm FZ C, are the geologically oldest members of the family. Their numerous dental similarities suggest that the two lineages may have diverged possibly in the middle or early late Oligocene.

Wakaleo premolars

The reasons for the variability in the presence of the anterior upper premolars in *W. schouteni* are unclear. Studies of tooth abnormalities in marsupials indicate that missing teeth mostly occur in the region of the premolars (Archer 1975) and this variability may be an example of abnormal development. In QM F24680 and QM F57314 the alveoli for P^2 are completely absent and those for P^1 appear to be malformed, occurring as shallow, narrow troughs rather than the round, deep sockets such as occur in QM F23443. Both the former specimens have relatively large alveoli for P^3 , hence the loss of P^2 and the malformed/rudimentary, or possibly lost, P^1 , has probably occurred in response to hypertrophy of P^3 .

Wakaleo vanderleuerei also shows variation in the presence of its anterior premolar, which was originally identified as P^2 (Murray *et al.* 1987). In '*Priscileo*' *roskellyae*, *W. pitikantensis* and *W. schouteni*, P^1 occurs

approximately midway between the canine and P^3 , and P^2 abuts the base of P^3 . In the cranium of *W. vanderleueri* (CPC 26604), the sole premolar alveolus lies nearly midway along the diastema between the canine and P^3 . Considering the pattern evident in other thylacoleonids, it is probable that this alveolus corresponds to P^1 and that P^2 , normally situated at the base of P^3 , has been lost as a result of hypertrophy of P^3 .

The complete dental formula for *W. schouteni* is: $I^{1-3}/_{1-2} C^1/_0 P^{1-3}/_{2-3} M^{1-4}/_{1-4}$. However, as indicated by Archer & Dawson (1982), the homology of the single-rooted teeth that lie between the procumbent I_1 and P_3 in thylacoleonids is open to speculation. They may represent posterior incisors and a canine, or a canine and anterior premolars. In species of *Wakaleo*, the anteriormost alveolus with its slightly horizontal, anteriorly directed orifice is similar to that for an incisor such as occurs in the mandibles of many diprotodontian taxa. For this reason, it is here regarded to similarly represent an alveolus for an incisor.

Wakaleo morphocline

The *Wakaleo* lineage has been considered to represent a morphocline characterized by successive increase in size through time (Murray & Megirian 1990), although recently the position of *W. alcootaensis* as the terminal member of this cline has been questioned (Yates 2015). Previously, *Wakaleo oldfieldi* represented the earliest stage of this cline, being the smallest taxon and from assemblages (Kutjamarpu LF and Riversleigh FZ C assemblages) regarded to be older than those yielding other species of *Wakaleo*. At present, the age of the Kutjamarpu LF is unresolved. It shares taxa with Riversleigh's FZ B and FZ C and could be early or middle Miocene in age (Black *et al.* 2012). *Wakaleo pitikantensis* now represents the probable earliest stage of this cline because it is smaller than *W. schouteni*, which in turn is smaller than *W. oldfieldi*. In addition, both these smaller taxa have been recovered from sediments that are estimated to be older (i.e. late Oligocene) than those yielding *W. oldfieldi*.

Riversleigh's D Site maxilla, QM F23446, differs from all other *Wakaleo schouteni* specimens in lacking a fourth molar, a loss shared with *W. oldfieldi* which it also approaches in size. However, attempted manipulated occlusion with mandibles of *W. oldfieldi* (SAM P17925 and QM F20895) results in a very poor fit, the mandibles being significantly oversized. In contrast, occlusal fit with mandibles from the White Hunter LF is remarkably close. Further support for this maxilla's referral to *W. schouteni* includes its full complement of premolars (P^{1-3}) and the likelihood of age equivalence between D Site and the other Riversleigh FZ A deposits that have produced *W. schouteni* (Arena *et al.* 2015). The slightly greater size and robustness of QM F23446 and the combination of the plesiomorphic premolar and apomorphic molar features

alternatively suggest that it might represent an annectant form between *W. schouteni* and *W. oldfieldi* in the *Wakaleo* morphocline. Better, more complete specimens of this enigmatic taxon from D Site would be required to test these alternative possibilities.

Palaeoecology

The increase in size of the *Wakaleo* lineage through time is an example of Cope's rule (more or less that taxa within phylogenetic sequences show a tendency to increase in size through time). The reasons for this increase are thought to be related to changes in the availability and nature of the resources that are consumed (McNab 2010). Carnivorous lineages show a tendency to increase in size as they change from omnivory (small prey and plant matter) to hypercarnivory (mostly flesh: Van Valkenburgh *et al.* 2004). The increase in body size of *Wakaleo* is most likely linked to increases in body size of their prey such as the larger herbivores that co-existed during the Miocene. In turn, the latter were responding to changes in the vegetation that occurred as the continent became drier and cooler, at least during the latter part of the middle Miocene and into the late Miocene (McGowran & Li 1994). Species of the calf-sized diprotodontid genus *Neohelos*, which are also present in Riversleigh's faunal zones A–D, show a morphocline trend of increasing size through the Miocene (Black *et al.* 2013). Most mammalian hypercarnivore lineages exhibit an increase over time in size of the carnassial teeth (Radinsky 1981; Van Valkenburgh 1991) and often a reduction in size and number of the teeth on either side of the carnassials. The relatively larger trigon and talonid basins found in the cheekteeth of the earlier species of *Wakaleo* (*W. pitikantensis*, *W. schouteni* and *W. oldfieldi*) suggest that for these species, transverse slicing (involving an oblique horizontal motion of the dentary) was still an important function in food processing, and it is likely that these species were at least somewhat more omnivorous. The dentary of *W. schouteni* is also suggestive of omnivory because it is relatively shallow and is unlike that of hypercarnivores which have deep jaws (Van Valkenburgh 1999). The larger middle Miocene and late Miocene species, respectively *W. vanderleueri* and *W. alcootaensis*, exhibit an increase in length of the premolar ($P^3/_3$) and loss and/or reduction of the posterior molars. In the former, the crown of M_3 is reduced to a small longitudinal crest and the talonid basin is lost. In the latter, the cheektooth number has been reduced to two (Archer & Rich 1982; Yates 2015). These dental changes reflect a transition to hypercarnivory that appears to have been well established by the late Miocene.

Body mass estimate

Very few estimates have been made of the body mass of marsupial lions. Estimates for the Pleistocene species

Thylacoleo carnifex have used regression equations employing measures of postcranial circumference (Wroe *et al.* 1999) and endocranial volume (Wroe *et al.* 2003). Gillespie *et al.* (2016) used upper molar alveoli row length (UMRL) with regression equations of Myers (2001) to estimate the body mass of *Wakaleo schouteni* (*Wakaleo* sp. nov. in that analysis) and two other early Miocene thylacoleonids (*Microleo attenboroughi* and ‘*Priscileo*’ *roskellyae*). That analysis produced an estimate of 5.2 kg for *W. schouteni*. However, Myers (2001) indicated that these regressions probably result in underestimates for marsupial lions because of the latter’s unusual dentitions (i.e. lengthened third premolar and reduced molars). By comparison, the largest extant marsupial carnivore, the Tasmanian devil (*Sarcophilus harrisi*), which has a smaller skull (length = 132 mm; Jones 1997), has a body mass of 8.5 kg (mean values for males; Jones 1997) and the placental carnivore, the clouded leopard (*Neofelis nebulosa*), which has a similar skull length (145 mm; Christiansen & Kitchener 2010), has a weight range of 11.5–23 kg. Given its skull length of 164 mm, a body mass estimate of 5.2 kg for *Wakaleo schouteni* appears to be an underestimate.

Total skull length (TSL) has been used to determine body mass in many mammalian groups including rodents (Rinderknecht & Blanco 2008; Millien & Bovy 2010; Bertrand

et al. 2016), primates (Martin, R. D. 1990; Sears *et al.* 2008) and phocids (Churchill *et al.* 2014). Van Valkenburgh (1990) found TSL was the second best variable for estimating body mass in fossil mammalian carnivores. Myers (2001) also found that TSL was a good predictor for marsupials in general, but significantly so for diprotodontians. Our estimates of the body mass of *W. schouteni* based on TSL results in estimates of 22.6 kg and 24.0 kg. These estimates are four to five times greater than that obtained using UMRL and, compared with the body mass of other mammalian carnivores with similar skull lengths (e.g. the clouded leopard), are probably more realistic estimates of the body mass of *W. schouteni*. It is likely that *W. pitikantensis*, which is smaller than *W. schouteni* in all dental and most postcranial measurements, had a smaller body mass.

It is possible that *W. schouteni* and *W. pitikantensis* may have been arboreal or semi-arboreal given that the late Oligocene environments in which they occurred were likely to have been forested (Fig. 11). Palaeoecological analyses of vertebrate faunas of Riversleigh suggest that the habitat of the area in the late Oligocene was open forest and in the early Miocene, open forest or rainforest (Travouillon *et al.* 2009). Palynological and macrofossil plant remains from central Australia indicate the presence of rainforest and sclerophyllous vegetation in that region



Figure 11. Reconstruction of *Wakaleo schouteni* challenging the thylacinid *Nimbacinus dicksoni* over a kangaroo carcass in the late Oligocene forest at Riversleigh (illustration by Peter Schouten).

during this period (Byrne *et al.* 2011; Martin, H. 1990, 1998). The morphological features of their humeri add support to an arboreal/scansorial hypothesis. The short greater tubercle, broad lesser tubercle and rounded head of the humerus of *W. pitikantensis* are features that allow the shoulder girdle to have a large range of motion; reducing the height of the greater tubercle reduces the likelihood of impingement of the tendons of the shoulders' rotator cuff muscles during the reaching motion, i.e. when the upper arm is abducted and/or flexed. A broader lesser tubercle provides a larger attachment site and greater lever arm for the subscapularis muscle, a muscle which stabilizes the shoulder and helps hold the head of the humerus in the glenoid cavity (Argot 2001). These features are characteristic of the humerus of arboreal species such as the koala (*Phascolarctos cinereus*) and the spotted cuscus (*Spilogocus maculatus*; Lee & Carrick 1989; Heinsohn 2002). Functional morphological studies of the humerus of *W. pitikantensis* and *W. schouteni* are currently being undertaken to test these hypotheses.

Conclusions

Craniodental and postcranial material of a new marsupial lion, *Wakaleo schouteni* sp. nov., is described from the Riversleigh WHA. Although this taxon has not reduced/lost the anterior upper premolars, previously regarded to be diagnostic for *Wakaleo*, it exhibits other *Wakaleo* apomorphies of the skull and molars. Comparison of the holotype of *Priscileo pitikantensis* Rauscher, 1987 from the Ngapakaldi LF with *Wakaleo schouteni* sp. nov. and other *Wakaleo* species reveals apomorphies of the M² and similarities in humerus morphology that support its referral to *Wakaleo*. *Priscileo pitikantensis* is therefore regarded as a junior synonym of *Wakaleo pitikantensis* comb. nov. *Wakaleo schouteni* is distinguished from *W. pitikantensis* on the basis of its different proximal humerus morphology and larger size, being 10% larger in most dental measures. Markedly different sizes in a sample of humeri of *W. schouteni* suggest this species was sexually dimorphic. Retention of three upper premolars and four molars are symplesiomorphic features for *Wakaleo* and *Priscileo* but distinguish *W. pitikantensis* and *W. schouteni* from later species of this genus, all of which exhibit premolar and molar reduction. These two species are the most primitive members of the genus and indicate a pre-late Oligocene origin for the lineage.

Acknowledgements

Support for research at the Riversleigh WHA has come from Australian Research Council grants to M. Archer, S. Hand and K. Black (DP130100197, DE130100167, DP170101420) at the University of New South Wales, P. Creaser and the CREATE Fund, UNSW, Queensland

Parks and Wildlife Service, Xstrata Community Partnership Programme North Queensland, Outback at Isa, Mount Isa City Council, and the Waanyi people of north-west Queensland. For kindly providing access to specimens we would like to thank Gavin Dally of the Museum and Art Galleries of the Northern Territory, Neville Pledge, Jim McNamara and Mary-Anne Binnie of the South Australian Museum, and Robert Jones of the Australian Museum. For their careful and expert preparation of the material we thank Henk Godthelp, Karen Black and the staff of the Vertebrate Palaeontology Laboratory, UNSW, and John Scanlon and Benita Chambers at the Riversleigh Fossil Laboratory of Outback at Isa. We also thank the many enthusiastic volunteers who have contributed to Riversleigh research in the field and in the lab. We thank K. H. Black for helpful comments on an earlier version of the manuscript.

Supplemental data

Supplemental material for this article can be accessed at: <https://doi.org/10.1080/14772019.2017.1391885>

References

- Aplin, K. 1990. *Basicranial regions of diprotodontian marsupials: anatomy, ontogeny and phylogeny*. Unpublished PhD thesis, The University of New South Wales, Sydney, 390 pp.
- Archer, M. 1975. Abnormal dental development and its significance in dasyurids and other marsupials. *Memoirs of the Queensland Museum*, **17**, 251–265.
- Archer, M. 1976a. The basicranial region of marsupi-carnivores (Marsupialia), interrelationships of carnivorous marsupials, and affinities of the insectivorous peramelids. *Zoological Journal of the Linnean Society, London*, **59**, 217–322.
- Archer, M. 1976b. The dasyurid dentition and its relationships to that of Didelphids, Thylacynids, Borhyaenids (Marsupialia) and Peramelids (Peramelina: Marsupialia). *Australian Journal of Zoology*, Suppl. Series No. **39**.
- Archer, M. 1984. The Australian marsupial radiation. Pp. 633–808 in M. Archer & G. Clayton (eds) *Vertebrate zoogeography and evolution in Australia*. Hesperion Press, Perth.
- Archer, M. & Dawson, L. 1982. Revision of marsupial lions of the genus *Thylacoleo* Gervais (Thylacoleonidae: Marsupialia) and thylacoleonid evolution in the late Cainozoic. Pp. 477–494 in M. Archer (ed.) *Carnivorous marsupials*. Royal Zoological Society of New South Wales, Sydney.
- Archer, M. & Rich, T. H. 1982. Results of the Ray E. Lemley Expeditions. *Wakaleo alcootaensis* n. sp. (Thylacoleonidae: Marsupialia), a new marsupial lion from the Miocene of the Northern Territory, with a consideration of the early radiation of the family. Pp. 495–502 in M. Archer (ed.) *Carnivorous marsupials*. Royal Zoological Society of New South Wales, Sydney.
- Archer, M., Godthelp, H., Hand, S. J. & Megirian, D. 1989. Fossil mammals of Riversleigh, northwestern Queensland: preliminary overview of biostratigraphy, correlation and environmental change. *The Australian Zoologist*, **25**, 29–65.

- Archer, M., Hand, S. J. & Godthelp, H.** 1994. *Riversleigh: The story of animals in ancient rainforests of inland Australia*. 2nd edition. Reed Books, Sydney, 264 pp.
- Archer, M., Hand, S. J., Godthelp, H. & Creaser, P.** 1997. Correlation of the Cainozoic sediments of the Riversleigh World Heritage fossil property, Queensland, Australia. Pp. 131–152 in J.-P. Aguilar, S. Legendre & J. Michaux (eds) *Actes du Congrès Biochrom '97*. Mémoires et Travaux de l'École Pratique des Hautes Études, Institut de Montpellier, Montpellier 21.
- Arena, D.** 2004. *The geological history and development of the terrain at the Riversleigh World Heritage Area during the middle tertiary*. Unpublished PhD thesis, The University of New South Wales, Sydney, 275 pp.
- Arena, D. A., Travouillon, K. J., Beck, R. M. D., Black, K. H., Gillespie, A. K., Myers, T. J., Archer, M. & Hand, S. J.** 2015. Mammalian lineages and the biostratigraphy and biochronology of Cenozoic faunas from the Riversleigh World Heritage Area, Australia. *Lethaia*, **49**, 43–60.
- Argot, C.** 2001. Functional-adaptive anatomy of the forelimb in the Didelphidae, and the paleobiology of the Paleocene marsupials *Mayulestes ferox* and *Pucadelphys andinus*. *Journal of Morphology*, **247**, 51–79.
- Bertrand, O. C., Schillaci, M. A. & Silcox, M. T.** 2016. Cranial dimensions as estimators of body mass and locomotor habits in extant and fossil rodents. *Journal of Vertebrate Paleontology*, **36**, e1014905.
- Black, K. H., Archer, M., Hand, S. J. & Godthelp, H.** 2012. The rise of Australian marsupials: A synopsis of biostratigraphic, phylogenetic, palaeoecologic and palaeobiogeographic understanding. Pp 983–1078 in J. Talent (ed.) *Earth and Life*. Springer Science+Business Media, Dordrecht.
- Black, K. H., Archer, M., Hand, S. J. & Godthelp, H.** 2013. Revision in the diprotodontid marsupial genus *Neohelos*: Systematics and biostratigraphy. *Acta Palaeontologica Polonica*, **58**, 679–706.
- Byrne, M., Steane, D. A., Joseph, L., Yeates, D. K., Jordan, G. J., Crayn, D., Aplin, K., Cantrill, D. J., Cook, L. G., Crisp, M. D., Keogh, J. S., Melville, J., Moritz, C., Porch, N., Sniderman, J. M. K., Sunnucks, P. & Weston, P. H.** 2011. Decline of a biome: evolution, contraction, fragmentation, extinction and invasion of the Australian mesic zone biota. *Journal of Biogeography*, **38**, 1635–1656.
- Christiansen, P. & Kitchener, A. C.** 2010. A neotype of the clouded leopard (*Neofelis nebulosa* Griffith 1821). *Mammalian Biology*, **76**, 325–331.
- Churchill, M., Clementz, M. T. & Kohno, N.** 2014. Predictive equations for the estimation of body size in seals and sea lions (Carnivora: Pinnipedia). *Journal of Anatomy*, **225**, 232–245.
- Clemens, W. A. & Plane, M.** 1974. Mid-Tertiary Thylacoleonidae (Marsupialia, Mammalia). *Journal of Paleontology*, **48**, 652–660.
- Crosby, K. & Norris, C. A.** 2003. Periotic morphology in the Trichosurin possums *Strigocuscus celebensis* and *Wyulda squamicaudata* (Diprotodontia, Phalangeridae) and a revised diagnosis of the tribe Trichosurini. *American Museum Novitates*, **3414**, 1–14.
- Finch, M. E. & Freedman, L.** 1982. An odontometric study of the species of *Thylacoleo* (Thylacoleonidae, Marsupialia). Pp 553–561 in M. Archer (ed.) *Carnivorous marsupials*. Volume 2. Royal Zoological Society of New South Wales, Surrey Beatty & Sons, Sydney.
- Flower, W. H.** 1867. On the development and succession of teeth in the Marsupialia. *Philosophical Transactions of the Royal Society, London*, **157**, 631–641.
- Gill, T.** 1872. Arrangement of the families of mammals with analytical tables. *Smithsonian Miscellaneous Collections*, **11**, 1–98.
- Gillespie, A.** 1997. *Priscileo roskellyae* sp. nov. (Thylacoleonidae, Marsupialia) from the Oligocene-Miocene of Riversleigh, northwestern Queensland. *Memoirs of the Queensland Museum*, **41**, 321–327.
- Gillespie, A. K.** 2007. *Diversity and systematics of marsupial lions from the Riversleigh World Heritage Area and the evolution of the Thylacoleonidae*. Unpublished PhD thesis. School of Biological, Earth and Environmental Sciences, University of New South Wales, Sydney, 394 pp.
- Gillespie, A. K., Archer, M., Hand S. J. & Black, K.** 2014. New material referable to *Wakaleo* (Marsupialia: Thylacoleonidae) from the Riversleigh World Heritage Area, northwestern Queensland: revising species boundaries and distributions in Oligo/Miocene marsupial lions. *Alcheringa*, **38**, 513–527.
- Gillespie, A. K., Archer, M. & Hand S. J.** 2016. A tiny new marsupial lion (Marsupialia, Thylacoleonidae) from the early Miocene of Australia. *Paleontologia Electronica*, **19.2** 29A, 1–25.
- Heinsohn, T. E.** 2002. Observations of probable camouflaging behaviour in a semi-commensal common spotted cuscus *Spiloglossus maculatus maculatus* (Marsupialia: Phalangeridae) in New Ireland, Papua New Guinea. *Australian Mammalogy*, **24**, 243–246.
- Illiger, C.** 1811. *Prodromus Systematis Mammalian et Avian Additus Terminis Zoographicis utriusque Classis*. C. Salzfild, Berlin, xviii + 301 pp.
- Jarman, P. J.** 1989. Sexual dimorphism in Macropodoidea. Pp. 433–447 in G. Grigg, P. J. Jarman & I. Hume (eds) *Kangaroos, wallabies, rat-kangaroos*. Surrey Beatty & Sons, Sydney.
- Jones, M.** 1997. Character displacement in Australian dasyurid carnivores: size relationships and prey size patterns. *Ecology*, **78**, 2569–2587.
- Lee, A. K. & Carrick, F. N.** 1989. Phascolarctidae. Pp. 740–754 in D. W. Walton & B. J. Richardson (eds) *Fauna of Australia; Mammalia*. Vol. 1B. Australian Government Printing Service, Canberra.
- Martin, H.** 1990. The palynology of the Namba Formation in the Wooltana-1 bore, Callabonna Basin (Lake Frome), South Australia, and its relevance to Miocene grasslands in central Australia. *Alcheringa*, **14**, 247–255.
- Martin, H.** 1998. Tertiary climatic evolution and the development of aridity in Australia. *Proceedings of the Linnean Society of New South Wales*, **119**, 115–136.
- Martin, R. D.** 1990. *Primate origins and evolution: a phylogenetic reconstruction*. Chapman and Hall, London, 804 pp.
- McGowran, B. & Li, Q.** 1994. The Miocene oscillation in southern Australia. *Records of the South Australian Museum*, **27**, 197–212.
- McNab, B. K.** 2010. Geographic and temporal correlations of mammalian body size reconsidered: a resource rule. *Oecologia*, **164**, 13–23.
- Megirian, D.** 1986. The dentary of *Wakaleo vanderleueri* (Thylacoleonidae: Marsupialia). *The Beagle*, **3**, 71–79.
- Millien, V. & Bovy, H.** 2010. When teeth and bones disagree: body mass estimation of a giant extinct rodent. *Journal of Mammalogy*, **91**, 11–18.
- Murray, P. & Megirian, D.** 1990. Further observations on the morphology of *Wakaleo vanderleueri* (Marsupialia: Thylacoleonidae) from the mid-Miocene Camfield Beds, Northern Territory. *The Beagle*, **7**, 91–102.

- Murray, P., Wells, R. & Plane, M.** 1987. The cranium of the Miocene thylacoleonid, *Wakaleo vanderleueri*: click go the shears – a fresh bite at thylacoleonid systematics. Pp. 433–466 in M. Archer (ed.) *Possums and opossums: studies in evolution*. Surrey Beatty and Sons and the Royal Zoological Society of New South Wales, Sydney.
- Myers, T. J.** 2001. Prediction of marsupial body mass. *Australian Journal of Zoology*, **49**, 99–118.
- Owen, R.** 1859. On the fossil mammals of Australia. Part 1. Description of a mutilated skull of a large marsupial carnivore (*Thylacoleo carnifex*, Owen) from a calcareous conglomerate stratum, eighty miles s.w. of Melbourne, Victoria. *Philosophical Transactions of the Royal Society, London*, **149**, 309–322.
- Owen, R.** 1866. On the fossil animals of Australia. Part 2. Description of an almost entire skull of the *Thylacoleo carnifex*, Owen, from a freshwater deposit, Darling Downs, Queensland. *Philosophical Transactions of the Royal Society, London*, **156**, 73.
- Radinsky, L. B.** 1981. Evolution of skull shape in carnivores; 1. Representative modern carnivores. *Biological Journal of the Linnean Society*, **15**, 369–388.
- Rauscher, B.** 1987. *Priscileo pitikantensis*, a new genus and species of thylacoleonid marsupial (Marsupialia: Thylacoleonidae) from the Miocene Etadunna Formation, South Australia. Pp. 423–432 in M. Archer (ed.) *Possums and opossums: studies in evolution*. Surrey Beatty and Sons and the Royal Zoological Society of New South Wales, Sydney.
- Rinderknecht, A. & Blanco, R. E.** 2008. The largest fossil rodent. *Proceedings of the Royal Society, Series B*, **275**, 923–928.
- Sears, K. E., Finarelli, J. A., Flynn, J. J. & Wyss, A. R.** 2008. Estimating body mass in New World “monkeys” (Platyrrhini, Primates), with a consideration of the Miocene platyrrhine, *Chilecebus carrascoensis*. *American Museum Novitates*, **3617**, 1–29.
- Swofford, D. L.** 2002. *PAUP. Phylogenetic analysis using parsimony (*and other methods)*. Version 4 (updated to 10 beta). Sinauer Associates, Sunderland, MA, 142 pp.
- Travouillon, K. J., Archer, M., Hand, S. J. & Godthelp, H.** 2006. Multivariate analyses of Cainozoic mammalian faunas from Riversleigh, northwestern Queensland. *Alcheringa*, Special Issue 1, 323–349.
- Travouillon, K. J., Legendre, S., Archer, M. & Hand, S. J.** 2009. Palaeoecological analyses of Riversleigh’s Oligo–Miocene sites: Implications for Oligo–Miocene climate change in Australia. *Palaeogeography, Palaeoclimatology, Palaeoecology*, **276**, 24–37.
- Travouillon, K. J., Gurovich, Y., Muirhead, J. & Beck, R. M. D.** 2010. An exceptionally well-preserved short-snouted bandicoot (Marsupialia: Peramelemorphia) from Riversleigh’s Oligo–Miocene deposits, northwestern Queensland, Australia. *Journal of Vertebrate Paleontology*, **30**, 1528–1546.
- Travouillon, K. J., Escarguel, G., Legendre, S., Archer, M. & Hand, S. H.** 2011. The use of MSR (minimum sample richness) for sample assemblage comparisons. *Paleobiology*, **37**, 696–709.
- Van Dyck, S. & Strahan, R.** 2008. *The Mammals of Australia*. Reed New Holland, Sydney, 887 pp.
- Van Valkenburgh, B.** 1990. Skeletal and dental predictors of body mass in carnivores. Pp. 181–205 in J. Damuth & B. J. MacFadden (eds) *Body size in mammalian paleobiology: estimation and biological implications*. Cambridge University Press, Cambridge.
- Van Valkenburgh, B.** 1991. Iterative evolution of hypercarnivory in canids (Mammalia: Carnivora): evolutionary interactions among sympatric predators. *Paleobiology*, **17**, 340–362.
- Van Valkenburgh, B.** 1999. Major patterns in the history of carnivorous mammals. *Annual Review of Earth and Planetary Sciences*, **27**, 463–493.
- Van Valkenburgh, B., Wang, X. & Damuth, J.** 2004. Cope’s rule, hypercarnivory, and extinction in North American canids. *Science*, **306**, 101–104.
- Woodburne, M. O.** 1984. Families of marsupials: relationships, evolution and biogeography. Pp. 48–71 in T. W. Broadhead (ed.) *Mammals: notes for a short course*. University of Tennessee Department of Geological, Sciences Studies in Geology, Volume 8.
- Woodburne, M. O., Macfadden, B. J., Case, J. A., Springer, M. S., Pledge, N. S., Power, J. D., Woodburne, J. M. & Springer, K. B.** 1993. Land mammal biostratigraphy and magnetostratigraphy of the Etadunna Formation (Late Oligocene) of South Australia. *Journal of Vertebrate Paleontology*, **13**, 483–515.
- Woodhead, J., Hand, S. J., Archer, M., Graham, I., Sniderman, K., Arena, D. A., Black, K. H., Godthelp, H., Creaser, P. & Price, E.** 2016. Developing a radiometrically-dated sequence for Neogene biotic change in Australia, from the Riversleigh World Heritage Area of Queensland. *Gondwana Research*, **29**, 153–167.
- Wroe, S.** 1999. The geologically oldest dasyurid, from the Miocene of Riversleigh, north-west Queensland. *Palaeontology*, **42**, 501–527.
- Wroe, S., Myers, T. J., Wells, R. T. & Gillespie, A.** 1999. Estimating the weight of the Pleistocene marsupial lion, *Thylacoleo carnifex* (Thylacoleonidae: Marsupialia): implications for the ecomorphology of a marsupial super-predator and hypotheses of impoverishment of Australian marsupial carnivore faunas. *Australian Journal of Zoology*, **47**, 489–498.
- Wroe, S., Myers, T. J., Seebacher, F., Kear, B., Gillespie, A., Crowther, M. & Salisbury, S.** 2003. An alternative method for predicting body mass: the case of the Pleistocene marsupial lion. *Paleobiology*, **29**, 403–411.
- Yates, A. M.** 2015. New craniodental remains of *Wakaleo alcootaensis* (Marsupialia; Thylacoleonidae) a carnivorous marsupial from the late Miocene Alcoota Local Fauna of the Northern Territory, Australia. *Peer J*, 3:e1408, doi: 10.7717/peerj.1408.